magnetochemistry

MDPI

Review

Exploring the Utilization of Magnetic Composite Materials for High-Risk Contaminant Removal from Wastewater by Adsorption and Catalytic Processes—A Review

Oana-Georgiana Dragos-Pinzaru, Nicoleta Lupu, Horia Chiriac and Gabriela Buema *

National Institute of Research and Development for Technical Physics, 47 Mangeron Boulevard, 700050 Iasi, Romania; odragos@phys-iasi.ro (O.-G.D.-P.); nicole@phys-iasi.ro (N.L.); hchiriac@phys-iasi.ro (H.C.)
* Correspondence: gbuema@phys-iasi.ro

Abstract: In the context of waters polluted with different high-risk contaminants, the development of efficient materials able to efficiently clean them is necessary. In the first part, the present review focuses on the ability of various types of magnetic layered double hydroxide materials to act as adsorbents for water contaminated mainly with heavy metals and dyes. Also, this paper reviews the ability of different magnetic layered double hydroxide materials to act as potential adsorbents for the treatment of wastewater contaminated with other types of pollutants, such as pharmaceutical products, phenolic compounds, phytohormones, and fungicides. In the second part, the applicability of the catalytic method for water depollution is explored. Thus, the use of simple or composite materials based on Fe_3O_4 is reviewed for the purpose of the catalytic degradation of organic compounds (dyes/phenols/pharmaceuticals). At the end, a review of multifunctional materials able to simultaneously neutralize different types of pollutants from wastewater is provided.

Keywords: magnetic composite materials; depollution; high-risk contaminants; adsorption process; catalytic process

check for updates

Citation: Dragos-Pinzaru, O.-G.; Lupu, N.; Chiriac, H.; Buema, G. Exploring the Utilization of Magnetic Composite Materials for High-Risk Contaminant Removal from Wastewater by Adsorption and Catalytic Processes—A Review. *Magnetochemistry* **2024**, *10*, 57. https://doi.org/10.3390/magnetochemistry10080057

Academic Editor: Carlos J. Gómez García

Received: 12 June 2024
Revised: 2 August 2024
Accepted: 7 August 2024
Published: 14 August 2024

Copyright: © 2024 by the authors. Licensee MDPI, Basel, Switzerland. This article is an open access article distributed under the terms and conditions of the Creative Commons Attribution (CC BY) license (https://creativecommons.org/licenses/by/4.0/).

1. Introduction

The contamination of water with substances referred to in the specialized literature as high-risk, dangerous, emerging, and hazardous contaminants/pollutants has negative impacts on human health and the environment. Various technologies for the treatment of contaminated waters, e.g., coagulation, flocculation, ultrafiltration, adsorption, ion exchange, and chemical precipitation, have been proposed. The adsorption process is the most widely used technique for water depollution due to its simple operation, large-scale application in industrial production, and minimal energy consumption. The adsorption approach is defined as "a process in which a substance that is in a liquid phase (called adsorbate) accumulates on a solid surface (namely adsorbent)" [1]. The influences of different experimental factors, such as solution pH, adsorbent dose, contact time, initial concentration of the pollutant, and temperature, are determined in order to establish the optimal parameters of the adsorption process. The pH of the solution and the dose of the adsorbent are some of the most important parameters of the adsorption process. Based on the experimental data obtained in the study of the influence of the initial concentration of the pollutant, adsorption isotherm models can be investigated, which are important since these models describe how an adsorbed particle interacts with an adsorbent. Moreover, based on the generated results, the design of the adsorption process can be established [1]. The literature presents different types of isotherms which can be used (Langmuir, Freundlich, Temkin, Dubinin–Radushkevich, Redlich–Peterson, Sips, Halsey, Harkin–Jura) [1], with the Langmuir and Freundlich isotherms being frequently applied in many studies.

Adsorption studies include kinetic and thermodynamic evaluations, as well. The kinetic models considered include the pseudo-first-order kinetic model, the pseudo-second-

order kinetic model, the intraparticle diffusion model, and the Elovich model [2], while the thermodynamic parameters investigated are Gibbs free energy (ΔG^0), enthalpy (ΔH^0), and entropy (ΔS^0) [3]. According to the information obtained by performing kinetic and thermodynamic studies, the nature of the adsorption process can be established [4].

The type of adsorbent is another important parameter of the adsorption process. So, the design of a non-toxic, low-cost, and environmentally friendly material is essential and continues to be a challenge for researchers. Furthermore, the ability of adsorbents to be regenerated and reused is an important characteristic of the adsorption process.

Previous studies have suggested two types of low-cost materials based on unmodified layered double hydroxides and unmodified magnetic nanoparticles, Fe_3O_4, as potential adsorbents for wastewater treatment.

Layered double hydroxides (LDHs), known as anionic clays or hydrotalcites, are a category of inorganic materials with a layered structure [5]. LDHs were discovered in the early 20th century [6]. The chemical formula of LDHs is $\left[M^{2+}_{1-x}M^{3+}_{x}(OH)_2\right]^{x+}\left[\left(A^{n-}\right)_{x/n}mH_2O\right]^{x-}$, where M^{2+} (e.g., Mg^{2+}, Ca^{2+}, Zn^{2+}, Ni^{2+}, Fe^{2+}, Co^{2+}) and M^{3+} (e.g., Al^{3+}, Fe^{3+}, Cr^{3+}, La^{3+}, Ga^{3+}) represent divalent metal ions and trivalent metal ions, respectively; x is the molar ratio of $M^{3+}/(M^{2+}+M^{3+})$, with values between 0.2 and 0.33 (M^{2+}/M^{3+} molar ratios of 2/1, 3/1, 4/1); A^{n-} represents interlayer anions, which include CO_3^{2-}, SO_4^{2-}, NO_3^-, Cl^-, and OH^-; and m is the number of water molecules in the layered structure [7]. LDHs can be prepared by various methods, such as the sol–gel method [8,9], the hydrothermal method [10–12], and the co-precipitation method. The co-precipitation method is the most involved technique for the synthesis of LDH materials [13–16]. High- or low-supersaturation conditions can be used for preparation [17], and low supersaturation is usually used for LDH synthesis. This method involves mixing a certain ratio of metal salt solutions, followed by the slow addition of precipitation agents. LDH material is obtained after aging during stirring [18]. The outstanding characteristics presented by LDHs are a well-ordered layered structure, a large surface area, excellent ion exchange properties, and a highly controllable composition [19]. Unfortunately, LDH materials are not easily separated from solution. The separation methods such as centrifugation or filtration are applied in order to obtain a clean supernatant (without adsorbent particles) so that the measurements are as accurate as possible.

Magnetite nanoparticles, Fe_3O_4, frequently synthesized by the co-precipitation method [20], are defined as "a ferrimagnetic mineral, with a face centered cubic inverse spinel structure which contains a combination of Fe^{2+} and Fe^{3+}" [21]. The main characteristics of magnetite nanoparticles, Fe_3O_4, are a "small particle size, large specific surface area, high reactivity, reversible adsorption behavior, which can be easily separated using an external magnetic field" [22].

Researchers have reported the ability of both unmodified LDHs and Fe_3O_4 to be used for wastewater treatment. For example, Hudcová and co-workers [23] synthesized Mg-Fe LDHs with different Mg/Fe molar ratios. The prepared adsorbents were applied for Zn(II) and Pb(II) removal. An investigation conducted by Tran and co-workers [24] demonstrated that MgAl-LDH material can remove Cu(II) and Pb(II). Zn–Al LDH and Mg–Fe LDH were prepared by Dalla-Nora and co-workers [25], and their adsorption potential for 2–nitrophenol (2–NP) removal was investigated. Adsorption capacities of 290 mg/g and 165 mg/g were obtained for Zn–Al LDH and Mg–Fe LDH [25]. Mg-Fe LDH with a Mg/Fe molar ratio of 2/1 was prepared by Awes and collaborators [26] as a potential adsorbent for Cu(II) ion removal. The results showed that the material removes this high-risk contaminant (165.16 mg/g) [26]. Abdel-Hady and collaborators [27] evaluated the ability of the Zn–Mg–Al layered double hydroxide in crystal violet dye removal, with a maximum adsorption capacity of 64.8 mg/g presented by the synthesized adsorbent. A study conducted by Alghamdi and collaborators [28] demonstrated that Cr(VI) ions can be removed using a Mg/Fe-LDH adsorbent. Iconaru and co-workers [29] have studied the ability of Fe_3O_4 (obtained by co-precipitation at room temperature) to remove Cu(II) and As(V) ions. The maximum adsorption capacities were 66.53 mg/g for

As(V) and 10.67 mg/g for Cu(II). The results of Zhang and collaborators [22] have showed that commercial Fe_3O_4 nanoparticles (purchased from Metal Powder Research Institute, China) can be used to remove the Cr(VI) and Cu(II) ions. The Fe_3O_4 nanoparticles can be reused for 6 cycles, without a visible reduction in the adsorption capacity.

Researchers have focused their studies on improving the adsorption capacities of raw LDHs and raw Fe_3O_4 materials, the number of studies increasing continuously. Due to the Coulombic attractive forces between positively charged LDH nanocomposites and negatively charged Fe_3O_4, a stable self-assembled magnetic composite material can be easily designed [30]. This new composite magnetic material, having a maximum number of active sites, high surface area, and high porosity, can be successfully used in environmental remediation [30]. The combination of LDH and Fe_3O_4 led to an enhanced adsorption capacity as compared to that of unmodified LDH_s and Fe_3O_4 materials. Additionally, these types of composite materials can be easily separated from solution using an external magnetic field.

The current review aims to present the most efficient and cheapest methods for water depollution reported in the literature. The first part of the review presents the ability of functionalized magnetic LDH-based composites to remove the high-risk contaminants from wastewaters by the adsorption process. The second part presents results of various research work focused on the study of the ability of magnetic compounds to be used as catalysts for water treatment.

2. Magnetic Composite Materials as Adsorbents and Catalysts

2.1. Functionalized Magnetic LDH-Based Composites as Adsorbents for High-Risk Contaminants Removal from Wastewaters

Various functionalized magnetic LDH-based composites for water depollution are presented in the literature. Based on the reported results, the ability of these composite materials to remove different categories of pollutants, mainly heavy metals and dyes, using the adsorption process is discussed in this section. The ability of different functionalized magnetic LDH-based composites as adsorbents for other type of pollutants, such as pharmaceutical products, phenolic compounds, phytohormone, and fungicides, is reviewed as well.

2.1.1. Heavy Metals Removal

The adsorption of Cu(II), Cd(II) and Pb(II) was carried out by using magnetic alginate microspheres based on Fe_3O_4/MgAl-LDH [31]. The data have demonstrated that the material shows good adsorption capacities, as follows: 64.66 mg/g for Cu(II), 74.06 mg/g for Cd(II), and 266 mg/g for Pb(II) ions.

According to the research results reported by Hou and co-workers [32] a magnetic layered double oxide/carbon composite of a spent adsorbent (magnetic MgAl-LDH after humic acid adsorption) can be recycled and successfully used for the removal of Cu(II), Cd(II), and Pb(II) ions. The maximum adsorption capacities of the adsorbent are 386.1 mg/g for Cd(II), 359.7 mg/g for Pb(II), and 192.7 mg/g for Cu(II) ions.

Behbahani and collaborators [33] have synthesized Fe_3O_4-$FeMoS_4$-based MgAl LDH adsorbents for the removal of the same three heavy metals: Pb(II), Cd(II), and Cu(II). The adsorption capacities were 190.75 mg/g for Pb(II), 140.50 mg/g for Cd(II), and 110.25 mg/g for Cu(II) using the following working parameters: pH 5, 60 min contact time, an adsorbent dosage of 0.03 g, and heavy metals concentrations between 10 to 300 mg/L.

The research conducted by our group [34] employed a magnetic material based on MgAl-LDH+Fe_3O_4 for Cd(II) ions removal as targeted the adsorbate. Additionally, the capacities of unmodified MgAl-LDH and Fe_3O_4 for the Cd(II) ions were also investigated. According to the obtained results, the highest adsorption capacity was obtained by using the MgAl-LDH+Fe_3O_4 composite (109.9 mg/g) followed by MgAl-LDH (91.7 mg/g), and by Fe_3O_4 (80.6 mg/g).

Li and co-workers [35] have synthesized a magnetic rhamnolipid-activated layered double hydroxides nanocomposite and have investigated its performance as adsorbent for simultaneous removal of Cu(II) ion and m-cresol. The results proved that the proposed adsorbent is suitable for this application.

Taheri and collaborators [36] have developed, characterized, and further applied Ca–Al LDH/Fe_3O_4 as a potential adsorbent for Cu(II) and Ni(II) ions. The maximum adsorption capacities were found to be 200 mg/g and 109.92 mg/g for Cu(II) and Ni(II), respectively. Moreover, the authors have investigated the possibility to use the magnetic adsorbent in real water (Shiraz industrial wastewater). The results have proved that Ca–Al LDH/Fe_3O_4 can be also used as an adsorbent for the treatment of the real water.

Mg/Fe LDH with Fe_3O_4-carbon spheres were designed and used for Cu(II) and Pb(II) ions removal, with the results showing that this formulated composite material presents good adsorption capacities for both ions: approx. 339 mg/g for Cu(II) and approx. 759.26 mg/g for Pb(II) [37].

Fe_3O_4@C@MgAl-LDH was synthesized by Zhang and co-workers [38], characterized and further tested as adsorbent for the Cr(VI) ion removal. The material shows an adsorption capacity of 152 mg/g at 40 °C and a solution pH of 6.

Fe_3O_4@Mg_xAl-LDH materials (x is the Mg/Al molar ratio of 2, 2.5, and 3) were synthesized by Sun and co-workers [39]. The representative scanning electron microscopy (SEM) and transmission electron microscopy (TEM) images of Fe_3O_4@Mg_xAl-LDH materials are depicted in Figure 1. According to their results, the LDH nanosheets remain flat on the surface of Fe_3O_4 nanoparticles in the case of the Fe_3O_4 @Mg_2Al-LDH (Figure 1a,b). A wool-ball-like hierarchical core–shell structure is obtained for the Fe_3O_4 @$Mg_{2.5}$Al-LDH material (Figure 1d,e), while a well-ordered and integrated core–shell structure is obtained for the Fe_3O_4 @Mg_3Al-LDH material (Figure 1g,h).

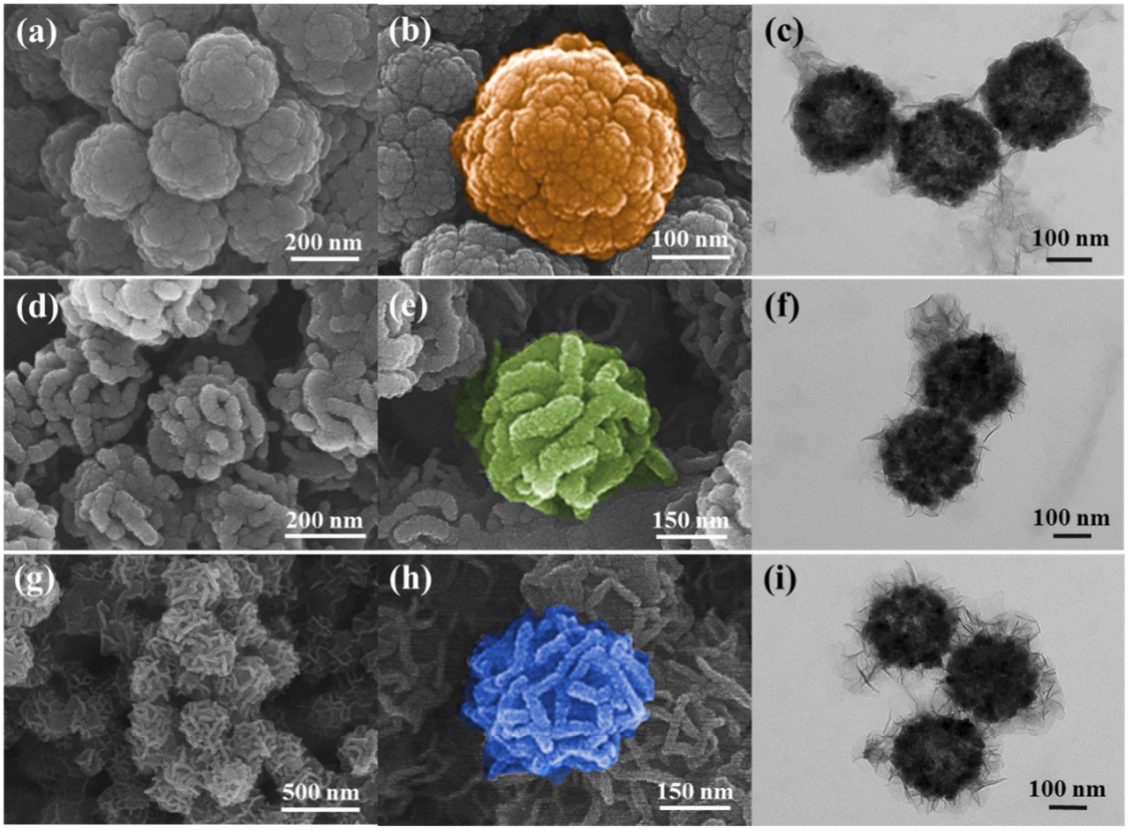


Figure 1. SEM images (**a**,**b**) and TEM image (**c**) of Fe_3O_4 @Mg_2Al-LDH; SEM images (**d**,**e**) and TEM image (**f**) of Fe_3O_4 @$Mg_{2.5}$Al-LDH; SEM images (**g**,**h**) and TEM image (**i**) of Fe_3O_4 @Mg_3Al-LDH. Source [39] with permission of Elsevier and Copyright Clearance Center.

The TEM investigation of Fe_3O_4 @Mg_2Al-LDH (Figure 1c) demonstrates the deposition and attachment of LDH nanosheets to the surface of Fe_3O_4 nanoparticles. The LDH nanosheets are not accumulated on the Fe_3O_4 nanoparticles and the high active surface area of Fe_3O_4 nanoparticles is maintained (Figure 1f,i). This behavior is attributed to the fact that LDH nanosheets are vertically dispersed on the surface of the Fe_3O_4 nanoparticles and extended outward.

The Fe_3O_4@Mg_XAl-LDH adsorbents were involved in the Cr(VI) ion removal process. A comparison between the adsorption properties of raw LDH, raw Fe_3O_4, and Fe_3O_4@Mg_xAl-LDH materials was performed. The obtained results have shown that the Fe_3O_4@Mg_3Al-LDH mixture manifests the highest adsorption capacity. The maximum adsorption capacity determined from the Langmuir isotherm model was found to be 108.7 mg/g.

Hong and co-workers [40] have presented a novel approach for in situ loading of Cu_2O nanoparticles onto Mg/Fe-LDH@Fe_3O_4. The adsorption capacity values, calculated by the pseudo second order kinetic model for Mg/Fe-LDH, Mg/Fe-LDH@Fe_3O_4, and Cu_2O materials are 29.89 mg/g, 48.33 mg/g, and 172.82 mg/g, respectively. The highest adsorption capacity was obtained for the Cu_2O@LDH@Fe_3O_4 3D multifunctional composite magnetic adsorbent, reaching 214.61 mg/g.

Zhao and co-workers have synthetized a composite material based on magnetic ZnAl-LDH [41] for the removal of Cr(VI) ions. The composite material is recommended for Cr(VI) ion removal based on the good adsorption capacity of approx. 197 mg/g. The regeneration study shows that the material can be reused 5 times.

Dinari and co-workers have reported the use of an adsorbent based on guar gum (GG)@Fe_3O_4@Ni/Al LDH for Cr(VI) adsorption [42]. The maximum adsorption capacity was 101 mg/g.

Kobylinska and co-workers [43] have proposed 2 types of magnetic composites based on Zn,Al-LDH intercalated with citric (Fe_3O_4/Zn,Al-LDH/Cit) and on Zn,Al-LDH intercalated with EDTA (Fe_3O_4/Zn,Al-LDH/EDTA) for the treatment of waters contaminated with U(VI). The results showed that, for a solution pH of 7.5, the maximum adsorption capacity of Fe_3O_4/Zn,Al-LDH/EDTA is visibly improved as compared to the maximum adsorption capacity of Fe_3O_4/Zn,Al-LDH/Cit.

The removal of Co(II) ion using the Fe_3O_4/MgAl-LDH composite material was studied by Shou and co-workers [44]. After synthesis, the composite was characterized by several methods and tested as a potential adsorbent. The study of the effect of contact time reveals that the process is very fast, with a removal efficiency of approx. 70% being achieved in 120 min. The regeneration study was performed for a number of 8 cycles of adsorption/desorption.

2.1.2. Dye Removal

An adsorbent based on Fe_3O_4@MgAl–LDH was synthesized and used for the removal of Congo red (CR) dye [45]. For comparison, the study was also performed on Fe_3O_4 and MgAl-LDH materials, with the results demonstrating that the Fe_3O_4@MgAl–LDH magnetic material presents an improved adsorption capacity (Figure 2). The study has also demonstrated the fact that the magnetic adsorbent can be reused, without significantly losing its adsorption capacity.

Wu and co-workers [46] have proposed the Fe_3O_4@MgAl-LDH for the CR dye removal. The composite adsorbent has a maximum adsorption capacity of approx. 404.6 mg/g, which is higher as compared to the maximum adsorption capacity of MgAl-LDH (345.72 mg/g) and Fe_3O_4 (220.56 mg/g). After 5 cycles of adsorption/desorption, the adsorption performance of the magnetic composite to remove the targeted pollutant decreases to 78.1%.

The study performed by F. Chengqian and collaborators [47] involved Cl^- intercalated Fe_3O_4@SiO_2@MgAl LDH nanocomposites for the removal of two anionic dyes, methyl orange (MO) and CR, and of a cationic dye, methylene blue (MB). The maximum adsorption

composite material capacities were 733 mg/g, 910 mg/g, and 385 mg/g for MO, CR and MB, respectively.

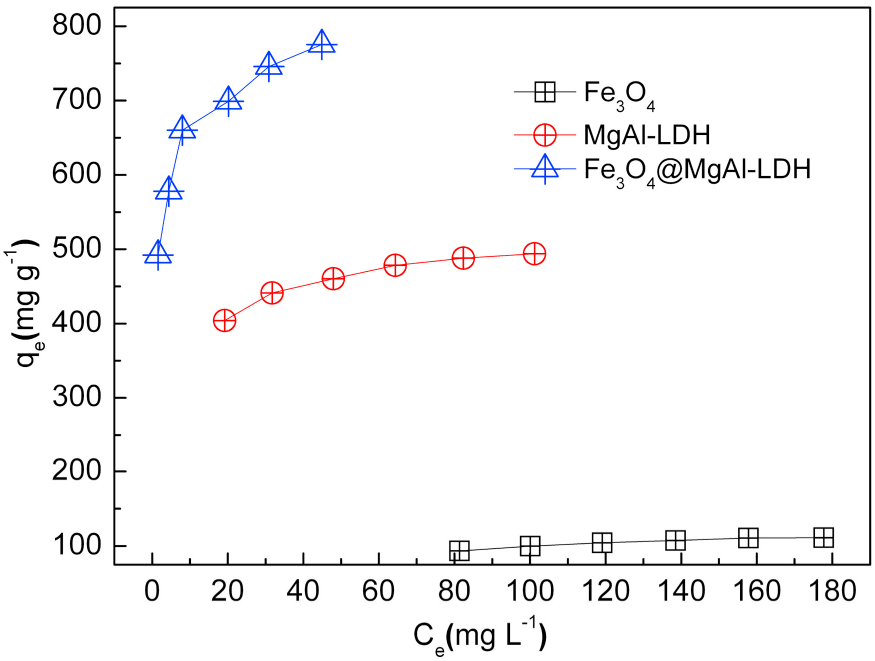


Figure 2. Adsorption isotherms of CR on Fe_3O_4, MgAl–LDH and Fe_3O_4@MgAl–LDH. Source [45] with permission of Elsevier and Copyright Clearance Center.

Sep@Fe_3O_4/ZnAl-LDH composite (Sep = Sepiolite) was proposed by Chengqian and co-workers [48] as adsorbent for MO and CR dyes removal. The composite material presents high adsorption capacities for both dyes. The adsorption mechanism of dyes is presented in Figure 3.

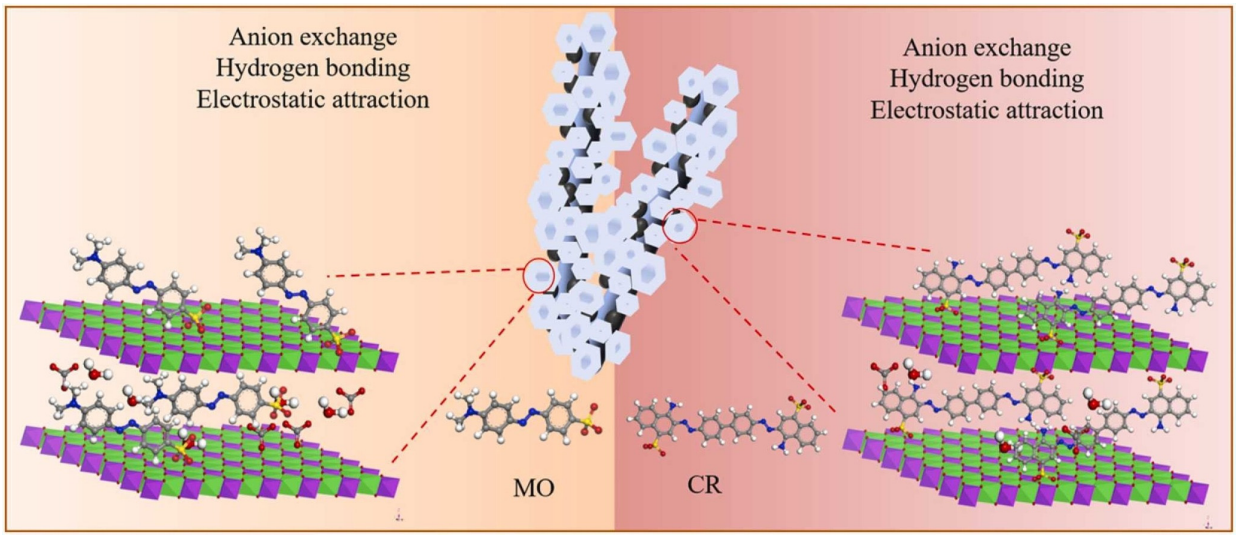


Figure 3. The proposed adsorption mechanism for dye removal. "This study demonstrated that Sep@Fe_3O_4/ZnAl-LDH provides a new idea for the development of a novel hierarchical magnetic pillared adsorbent for the efficient removal of anionic dyes". Source [48] with permission of Elsevier and Copyright Clearance Center.

MO dye removal was studied by Mallakpour and Hatami [49] by using LDH@Fe_3O_4/PVA adsorbent (LDH refers to MgAl type). The maximum adsorption capacity was 19.59 mg/g

under the following working parameters: solution pH = 6, adsorbent dosage = 0.1 g, initial MO concentration of 30 mg/L, contact time = 420 min, T = 298 K.

Fe_3O_4-PEG-Mg-Al-LDH nanocomposites (PEG = polyethylene glycol), with different molecular weights of PEG (2, 4, 6 k), were synthesized and characterized using various methods [50]. The maximum adsorption capacity values of the three prepared adsorbents for MO dye are 775.19 mg/g, 826.44 mg/g, and 833.33 mg/g.

A composite material based on Fe_3O_4/ZnCr-LDH was synthesized by Chen and co-workers [51] and tested for MO dye removal by adsorption processes:

- The kinetic study was carried out using Fe_3O_4/ZnCr-LDH composite at room temperature, 0.25 g/L adsorbent dosage, and 100 mg/L MO dye concentration. The contact time was between 5 min and 24 h. For comparison, the performance of ZnCr-LDH, Fe_3O_4, and an adsorbent obtained by physical mixture between Fe_3O_4 and ZnCr-LDH (abbreviated as Fe_3O_4+ ZnCr-LDH), was studied as well.
- Fe_3O_4/ZnCr-LDH and Fe_3O_4+ZnCr-LDH materials were used for the adsorption isotherm study. The adsorbent dosage was set at 0.25 g/L. The initial MO concentration varied from 50 mg/L to 500 mg/L.

The results showed that Fe_3O_4/ZnCr-LDH presents an improved adsorption capacity as compared to Fe_3O_4+ZnCr-LDH.

Li and co-workers [52] have prepared a magnetic core–shell dodecyl sulfate intercalated LDH (MgAl type) nanocomposite with the aim to establish its ability for a cationic type dye and an anionic type dye removal. The targeted cationic dye was MB, while the targeted anionic dye was MO. The authors have also investigated the adsorption in [MB dye + Cu(II) ion] or in [MO dye + Cu(II) ion] binary systems. Overall, the results showed that: (i) the adsorption capacity for MB dye has decreased in the presence of Cu(II) ion; and (ii) the adsorption capacity for MO dye increased in the presence of Cu(II) ion.

Recently, MB dye removal was studied by Khooni and co-workers [53] using a magnetic graphene oxide/Mg-Al LDH nanocomposite (abbreviated as MGO/LDH) based on magnetic graphene oxide (MGO) and Mg-Al LDH. The corresponding FE-SEM images and EDX are presented in Figure 4. The maximum adsorption capacity values of MGO/LDH varied from 11.6 mg/g to 58.8 mg/g.

A cross-linked magnetic LDH/GG bionanocomposite, where LDH is of Ni–Al type, was proposed as a potential adsorbent for MB dye removal by Tabatabaeian and co-workers [54]. The results of the study highlighted that the maximum adsorption capacity was 64.5 mg/g.

Magnetic ZnAl LDH was used for the adsorption of two dyes: a cationic type dye, namely malachite green (MG) and an anionic type dye, CR [55]. A series of parameters which impacted the adsorption ability were investigated. The magnetic composite adsorbent is able to remove 850.93 mg/g of MG and 279.09 mg/g of CR. The material has a good adsorption capacity, for both dyes, when using Na_2CO_3 (0.1 mol/L).

MG and CR removal was investigated by Liu and co-workers [56] using Fe_3O_4/MgAl-TA LDH. The authors found that the maximum adsorption capacities are 1520 mg/g for CR and 819 mg/g for MG. The Fe_3O_4/LDH was also used for neutral red dye removal (cationic dye type), the material showing a promising adsorption capacity of 929 mg/g at room temperature. Overall, the material can be used for the treatment of dye-contaminated waters, showing a good reusability. Moreover, the study was performed on real wastewater provided by a textile factory, with the aim of establishing the material's performance. The discoloration rate was 76.1% after 4 h of contact time.

Indigo carmine (IC) dye was removed from polluted water using a magnetic nanoadsorbent based on functionalized graphene oxide@gellan gum hydrogel @MnFe LDH [57]. A maximum adsorption capacity of 434.7 mg/g was achieved. The material can be reused up to 5 cycles, showing an adsorption efficiency of 95.1%.

Fe_3O_4/C/Co–Al LDH adsorbent was used for the treatment of waters contaminated with tartrazine and IC dyes [58]. The adsorption capacities presented by the composite were 52.3 mg/g for the TA dye and 61.7 mg/g for the IC dye.

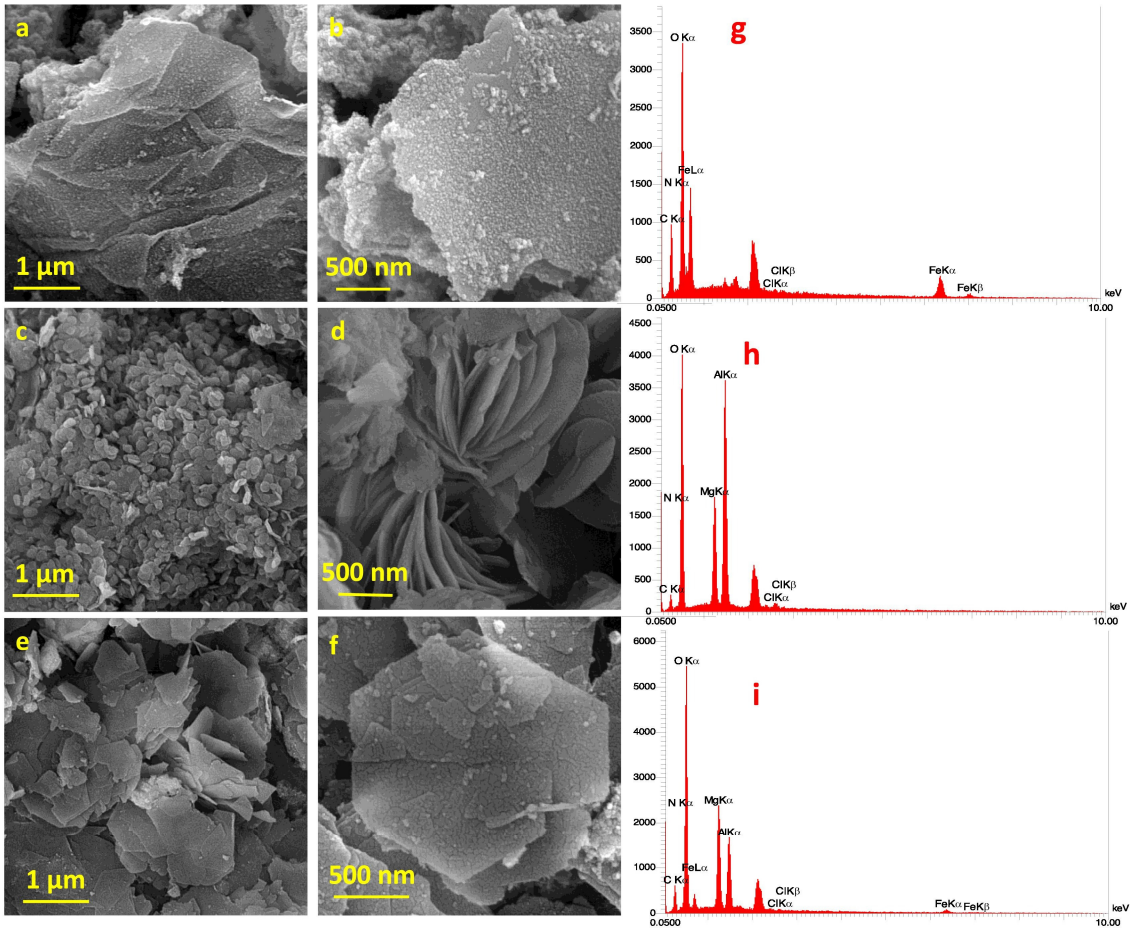


Figure 4. FE-SEM images of MGO (**a**,**b**), Mg-Al LDH (**c**,**d**), and MGO/LDH (**e**,**f**) in low (left column) and high (middle column) magnifications and their corresponding EDX (right column): of MGO (**g**), Mg-Al LDH (**h**), and MGO/LDH (**i**). Source [53] with permission of Elsevier and Copyright Clearance Center.

The Fe_3O_4/GO/Zn-Fe LDH material (where GO represents graphene oxide) was used for the removal of MB dye. Several working parameters were evaluated: pH (4–11), adsorbent dose (3–15 mg), contact time (2–60 min), and initial dye concentration (30–100 mg/L) with the aim to determine the optimal adsorption conditions [59]. The maximum adsorption capacity of the material was 322.58 mg/g (which is higher than of other similar adsorbents, as the authors stated). Moreover, the antibacterial efficiency of the adsorbent for Staphylococcus aureus (*S. aureus*) and Escherichia coli (*E. coli)* was evaluated, with promising results: *S. aureus* (75.09%) and *E. coli* (80.53%).

Kheradmand and co-workers [60] reported the adsorption capacity of a magnetic rhamnolipid-Co/Al for cationic and anionic dye removal. Their results have shown that the adsorption of MB dye is improved when a basic medium is used, while the adsorption of the anionic dye, reactive orange 16 (RO16), is improved when an acidic medium is used. The adsorption capacity values were found to be 54.01 mg/g for the MB dye and 53.04 mg/g for the RO16 dye, respectively.

Meira and collaborators [61] have prepared a magnetic MgAl-LDH (Mag-MgAl), and its surface is modified using 0.2 mol/L of sodium dodecyl sulfate (SDS). The obtained material was abbreviated as Mag-MgAl/SDS. The adsorbent was utilized for the treatment of waters contaminated with 2 type of dyes, namely ponceau red (PR) and MB. For comparison, the performance of Mag-MgAl material as a potential adsorbent was also tested. The study concluded that:

- Mag-MgAl/SDS material is recommended as adsorbent for MB dye removal.

- Mag-MgAl adsorbent is recommended as adsorbent for PR dye removal.
- The simultaneous removal of both dyes have demonstrated that Mag-MgAl/SDS has the ability to remove a higher quantity of MB dye; in contrast, the Mag-MgAl adsorbent has the ability to better remove PR dye.

Wastewaters contaminated with alizarin red S (AR) and alizarin yellow (AY) dyes were treated using Fe_3O_4/Zn-Al-Zr LDH. Four working parameters were investigated: solution pH, initial dye concentration, contact time, and Fe_3O_4/Zn-Al-Zr LDH dosage. The maximum adsorption capacity values in single and binary solutions were 150.87 mg/g and 130.21 mg/g for AR, and 166.85 mg/g and 145.35 mg/g for AY, respectively [62].

Adlnasab and co-workers reported the composite Fe_3O_4@MCM@Cu–Fe–LDH, prepared based on MCM-41 and LDH coated on magnetic nanoparticles, for the AY dye removal [63]. A maximum adsorption capacity of 121.95 mg/g was obtained.

Gonçalves and co-workers [64] carried out a study on magnetite/layered double hydroxide composite for the dye removal via adsorption, and Fenton and photo-Fenton processes. The targeted pollutants were reactive black 5 (RB5) and MB dyes. Regarding the removal of dyes using the adsorption technique, the investigation revealed that the prepared material had no high adsorption capacity of MB dye due to the positive electrostatic charge present in the cationic molecule. Therefore, the research group performed the adsorption kinetics study as well as the adsorption isotherms studies only for RB5. The Langmuir and Freundlich adsorption isotherms are depicted in Figure 5. The maximum adsorption capacities, according to Langmuir model, are: 30.347 mg/g (Fe_3O_4), 90.680 mg/g (CoCr-LDH), and 150.239 mg/g (Fe_3O_4/LDH).

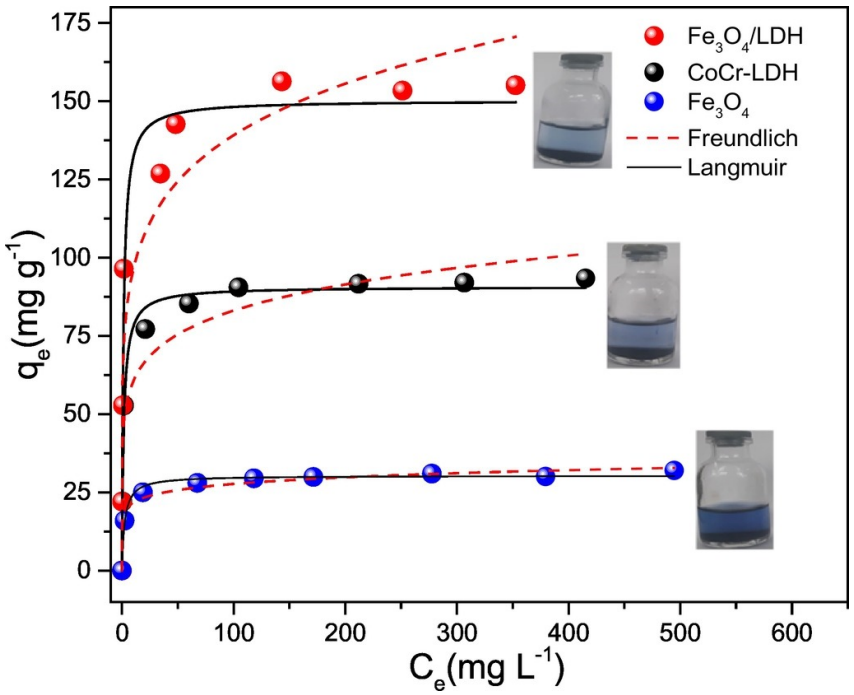


Figure 5. Langmuir and Freundlich adsorption isotherms. Source [64] with permission of Elsevier and Copyright Clearance Center.

The Fe_3O_4@SDBS@LDHs composite (where SDBS represents the sodium dodecyl benzene sulfonate and LDH refers to MgAl LDH-type) was used for the brilliant green (BG) dye removal [65]. The results have proved that the Fe_3O_4@SDBS@LDHs composite can successfully be used for the removal of BG dye. The maximum adsorption capacity values are 340.1 mg/g at 293K, 518.1 mg/g at 298K, and 819.6 mg/g at 303K.

Fuchsin acid dye removal was performed using a magnetic CaAl-LDH composite [66]. The adsorption capacity of the adsorbent was 36.86 mg/g.

2.1.3. Removal of Other Categories of Pollutants

Apart from applications for heavy metals and dye removal, the magnetic composite materials based on LDH and Fe_3O_4 have been investigated as potential adsorbents for other types of contaminants, such as: tetracycline, ibuprofen, oxytetracycline, levofloxacin, 2,4-dichlorophenol, glyphosate, para nitrophenol, 1-naphthalene acetic acid, phytohormone (indole-3-butyric acid), and fungicides.

The removal of ibuprofen using a core–shell magnetic rhamnolipid@Co/Al LDH was investigated by Kheradmand and co-workers [67]. The designed adsorbent presents a maximum adsorption capacity of ~200 mg/g. The reusability study has been performed for 4 cycles showing that the composite material can be successfully reused.

Smata and Yoshimura [68] formulated a magnetic layered double hydroxide for oxytetracycline removal from water, having an adsorption capacity of 217 mg/g and a good regeneration ability (over 80% of adsorption efficiency was maintained until the 5th cycle).

Levofloxacin antibiotic removal from polluted water was reported by Azqhandi and co-workers [69] using magnetic NiFe-LDH/N-MWCNTs nanocomposite materials. The material presents a good potential for removing this category of contaminant, 344.83–454.55 mg/g. The recyclability study was carried out for 7 cycles, with the results showing a decrease in the removal performance from 95.28% to 70.38%. Overall, the study highlighted the applicability of NiFe-LDH/N-MWCNT nanocomposites for levofloxacin antibiotic removal.

Kheradmand and co-workers [70] have used a magnetic bio-surfactant rhamnolipid-layered double hydroxide nanocomposite (where the layered double hydroxide refers to Co/Al type) for rifampin removal. Their objective was fully achieved considering that the maximum adsorption capacity presented by the designed composite is 221.3 mg/g for a low adsorbent dosage (0.67 g/L).

Apart from the PR and MB dye removal (see Section 2.1.2), Meira and co-workers [61] have proposed a magnetic LDH-based composite material treated with a SDS material (Mag-MgAl/SDS) for the removal of ciprofloxacin (CP). The results indicated that Mag-MgAl/SDS presents an improved adsorption capacity as compared to Mag-MgAl.

The magnetic composite prepared by Wu and co-workers [71], magnetic polyimide@Mg-Fe layered double hydroxide core–shell, was tested as a potential adsorbent for the removal of different types of high-risk contaminants, including tetracycline (TC), 2,4-dichlorophenol (2,4-DCP), and glyphosate (GP). According to the Langmuir isotherm model, the maximum adsorption capacity values are 185.53 mg/g (TC), 176.06 mg/g (2,4-DCP), and 190.84 mg/g (GP), at 298 K. The authors have also performed reusability studies(Figure 6). The results showed that after 5 cycles, the adsorption capacity values decreased from 51.11 mg/g to 41.17 mg/g (TC), from 35.22 mg/g to 25.59 mg/g (2,4-DCP), and from 145.21 mg/g to 115.83 mg/g (GP).

Khomeyrani and collaborators [10] have reported the possibility of using a magnetic composite material synthesized from graphite carbon nitride (g-CN), Fe_3O_4, and Ca-Al-LDH for para nitrophenol (PNP) adsorption. The investigated parameters were: the initial PNP concentration, temperature, dosage, and sonication time. The reusability study has indicated that the proposed adsorbent can be reused for 6 cycles. The overall results highlighted that this newly developed magnetic composite may be applied for the treatment of wastewaters contaminated with PNP pollutant.

Two adsorbents, namely magnetic CoMgAl LDH (C-MLDH) and magnetic FeMgAl LDH (F-MLDH), were synthesized, characterized, and further tested for the removal of 1-naphthoacetic acid (NAA) [72]. The representative SEM and TEM images for Fe_3O_4, C-MLDH, and F-MLDH are depicted in Figure 7. The results showed that both adsorbents can be successfully used for the removal of NAA.

A phytohormone, namely indole-3-butyric acid (IBA), was removed from polluted waters using composite magnetic layered double hydroxide-based adsorbents [73]. The authors have prepared the composite materials (MLDH-1, MLDH-2, and MLDH-3) through three different synthesis methods. The preliminary adsorption study has demonstrated that the MLDH-1 composite presents the highest adsorption capacity. Therefore, further

investigations were carried out using MLDH-1 adsorbent. The adsorption capacity of MLDH-1 for IBA removal was 522.6 mg/g.

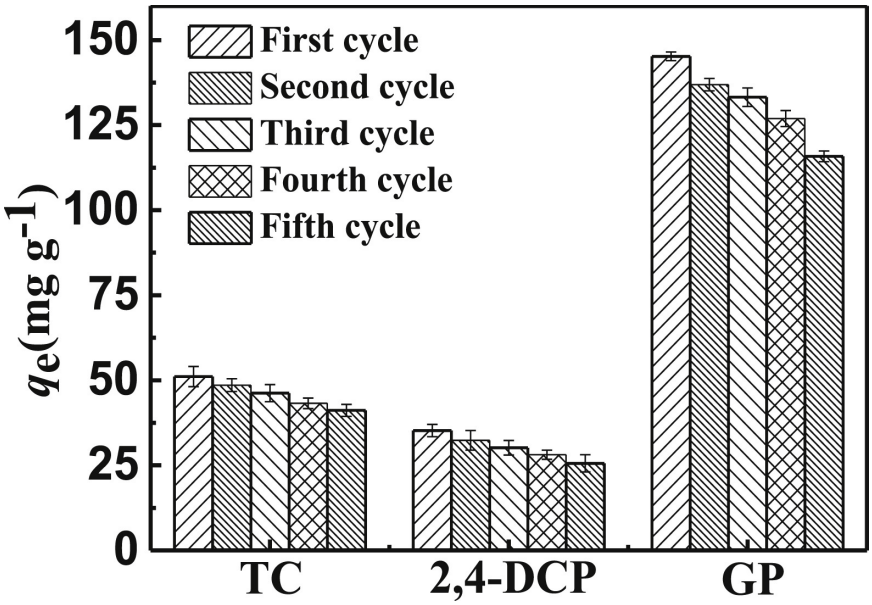


Figure 6. Effect of recycling times for the adsorption of TC, 2,4-DCP and GP on magnetic PI@LDO composites. Source [71] with permission of Elsevier and Copyright Clearance Center.

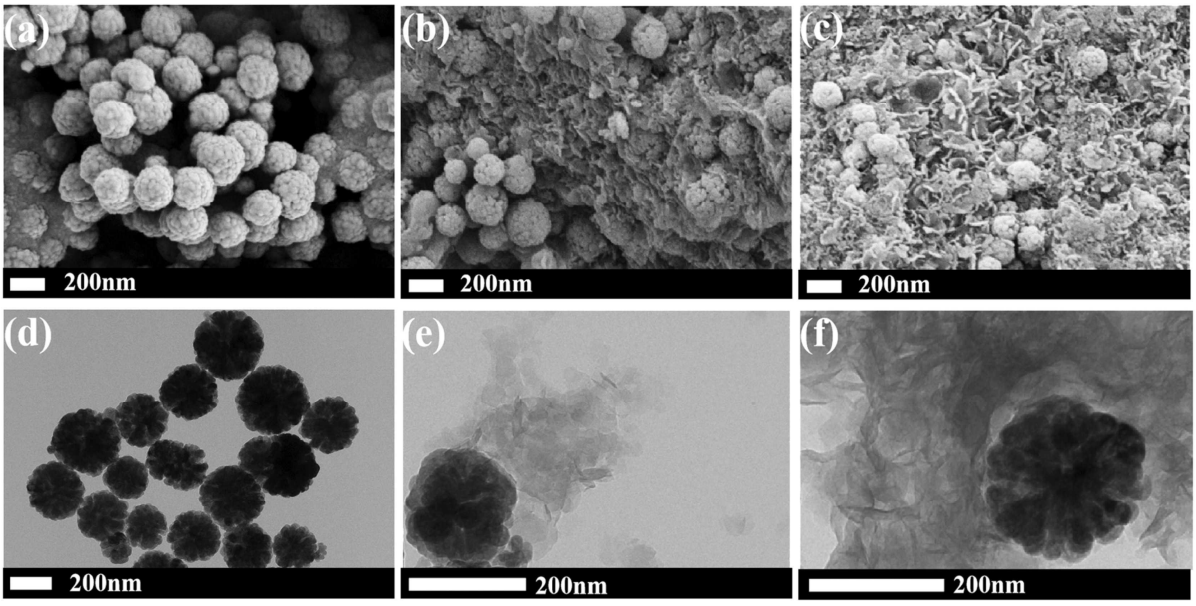


Figure 7. SEM (**a**–**c**) and TEM (**d**–**f**) images of Fe_3O_4 (**a**,**d**), C-MLDH (**b**,**e**), and F-MLDH (**c**,**f**). Source [72] with permission of Elsevier and Copyright Clearance Center.

Another category of high-risk contaminants with negative impact for environmental and for human health are the fungicides. Lu and co-workers [74] synthesized a novel magnetic composite, Fe_3O_4@Zn_2Al-LDH@MIL-53(Al), and used it for different azole fungicide removal. The results have demonstrated that the adsorbent presents adsorption capacities varying from 43.54 to 71.79 mg/g. Additionally, Fe_3O_4@Zn_2Al-LDH@MIL-53(Al) was tested as a potential adsorbent for the removal of fungicides in real water samples, with a removal efficiency above 95%.

2.2. Magnetic Compounds as Catalysts for Water Treatment

Another efficient method for removing dyes, antibiotics or phenolic compounds from contaminated waters is the use of the catalytic reaction for their complete degradation.

Heterogeneous high-efficiency oxidation processes (HE-AOPs) have been utilized to remove contaminants from wastewater. These procedures rely on the production of extremely reactive species that can degrade complex chemical polutant molecules, including hydroxyl radicals. The mechanism of the HE-AOP process consists of four important steps. In the first step, the water pollutants were adsorbed on a catalyst surface. Secondly, reactive species (such as hydroxyl radicals) were produced by activating the catalyst surface by an energy source (such as UV light). During the third step, reactive species, such as hydroxyl radicals, are produced and used in the next stage to achieve oxidation. Thus, the contaminants that have been adsorbed on the catalyst surface are the molecules subsequently broken down into less hazardous compounds by these reactive species. In the last step, the desorption process, the oxidized products are removed and the catalyst surface becomes ready for a new cycle.

Advanced oxidation processes, AOPs, employ light irradiation, catalysts, and oxidants to generate highly active species (such SO_4• and •OH radicals) that assist in the oxidation of organic materials. The molecules of the organic pollutants from the contaminated water will be destroyed by the radicals generated during the AOPs, by slowly oxidizing them into small molecules, that are either non-toxic or with low toxicity. The disadvantages of homogeneous AOPs, such as reduced stability, severe pH dependence, and poor catalyst recycling have been overcomed by heterogeneous catalytic AOPs, that have been used extensively in wastewater treatment. Figure 8 presents the principles of the heterogeneous high-efficiency oxidation process [75].

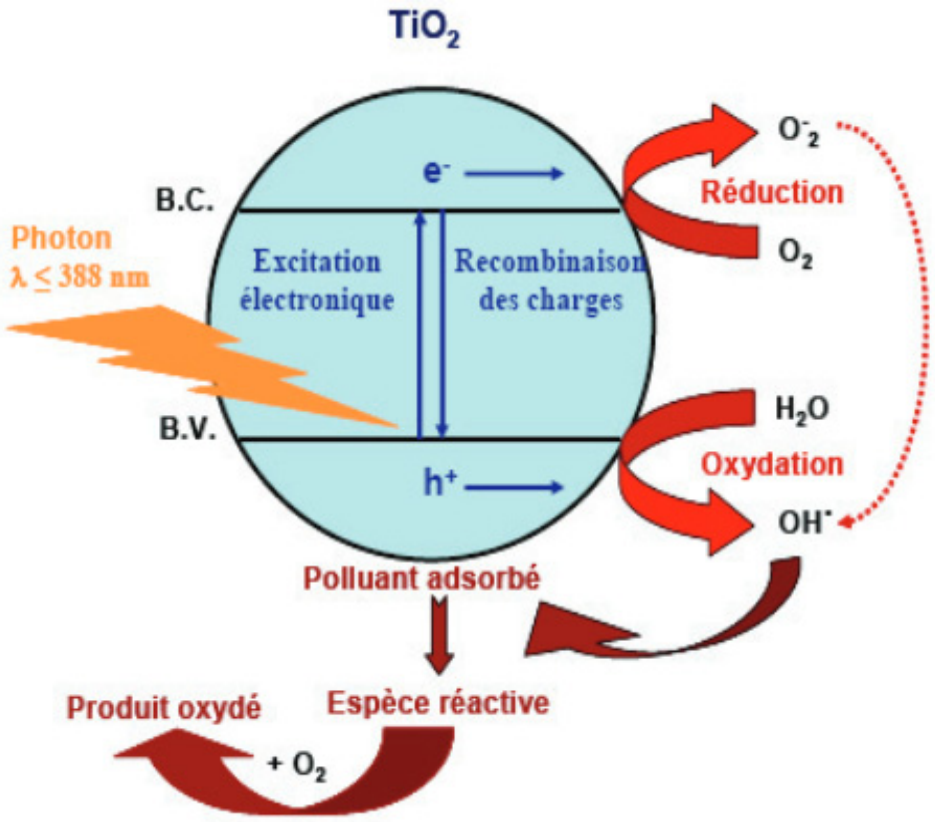


Figure 8. Schematic illustration of the heterogeneous high-efficiency oxidation process (Excitation électronique: electronic excitation; Recombinaison des charges: recombination of charge carriers; Reduction: reduction; Oxydation: oxidation; Polluant adsorbé: adsorbed pollutant; Espèce réactive: reactive species; Produit oxydé: oxidized product). Source [75] with permission of Elsevier and Copyright Clearance Center.

2.2.1. Dye Removal

MB dye degradation by heterogeneous Fenton oxidation was studied by Atta and co-laborators [76]. In their work, the ionic cross-linked 2-acrylamido-2-methylpropane sulfonic acid-co-acrylic acid hydrogel and AMPS/AA with Fe_3O_4 nanoparticles (AMPS/AA-Fe_3O_4 composites) have been prepared and tested for complete MB degradation. Thus, the MB was adsorbed by AMPS/AA and further degraded by Fenton oxidation using Fe_3O_4 as catalyst. The results showed that the degradation rate of MB by using AMPS/AA-Fe_3O_4 as a catalyst is 171 mg L^{-1} h^{-1}.

CR dye is a dangerous pollutant and removal has attracted the attention of the scientific community. Arora and co-workers [77] have prepared Cu-loaded Fe_3O_4@TiO_2 core shell nanoparticles and have studied their capacity to catalytically degrade the CR dye by the solar light-driven photodegradation. The catalyst is time, economical, and energy efficient, demonstrating a high rate of photodegradation under solar radiation, 96% in 10 min. The catalyst exibited nearly identical levels of activity after being magnetically separated five times (from 96 to 90%). TiO_2@Fe_3O_4-based catalysts were employed by Zhu and co-workers [78] for the removal of CR from wastewaters. More precisely, C-TiO_2@Fe_3O_4/AC composites were obtained by loading C-TiO_2 and Fe_3O_4 nanoparticles onto granular activated carbon (AC) and their catalytic activity for distruction of the azo bonds and aromatic rings in CR was analyzed. The results showed that the removal rate reached 92.9% after 30 min of simulated sunlight irradiation.

A novel promising Fenton-like catalyst Fe_3O_4@ZIF-67/CuNiMn-LDH, able to efficiently degrade the CR dye from wastewater, was developed by Eltaweil and co-workers [79]. The experiments have shown that the CR was 90.9% degraded by the Fe_3O_4@ZIF-67/Cu Ni Mn-LDH/H_2O_2 system within 30 min, in optimum conditions (solution pH = 5, 0.01 catalyst dosage, 500 mg/L H_2O_2 concentration, 50 mg/L CR concentration and 25 °C).

CeO_2/Fe_3O_4 magnetic catalysts were used by Xiang and collaborators [80] for the remediation of wastewaters polluted with CR dye. The composite material was used as a catalyst for CR degradation, by the photocatalysis-Fenton reaction, with a high catalytic capacity for 1000 mg/L CR.

The mechanism for CR dye removal was presented by Khan and co-workers in [81]. The reactions of the process are as follows:

$$Fe_3O_4@CS\ photocatalyst + h\nu \rightarrow Fe_3O_4@CS\ photocatalyst + \left(e^- + h^+\right) \quad (1)$$

$$e^- + O_2 \rightarrow O_2^{-\cdot} \quad (2)$$

$$O_2^{-\cdot} + CR\ dye \rightarrow CO_2 + H_2O \quad (3)$$

$$h^+ + H_2O \rightarrow OH^{-\cdot} + H^+ \quad (4)$$

$$OH^{-\cdot} + CR\ dye \rightarrow CO_2 + H_2O \quad (5)$$

The magnetite nanoparticles, simple or as composites, were also used as catalysts, for degradation processes, in order to purify waters polluted with MO dye. The magnetite nanoparticles, prepared by co-precipitation, exhibited a 98.3% removal of MO within 110 min [82].

A comparable removal rate (up to 99.24%) was obtained by Arshad and collaborators [83] using graphene/Fe_3O_4 nanocomposites as catalysts. The photo-Fenton-type reaction removal mechanism (presented schematically in Figure 9), indicated that the electrons from the valence band are photoexcited to the magnetite conduction band. Further, the graphene layers easily accepted these photoexcited carriers, giving them a convenient transit channel. The H_2O_2 adsorbed on the active sites provided by graphene could be more easily converted to hydroxyls (•OH) and hydroperoxyl radicals (•OOH), thanks to the accepted electrons.

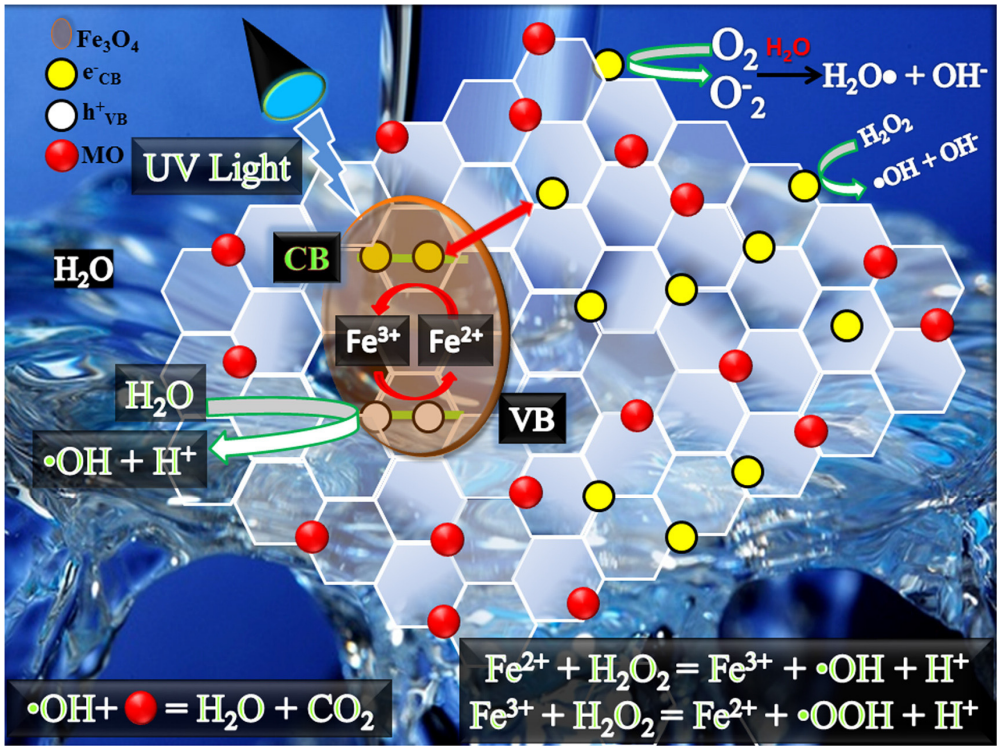


Figure 9. Schematic illustration of the photo-Fenton-type reaction mechanism of MO dye in the presence of Fe_3O_4 and graphene/Fe_3O_4 nanocomposite. Source [83] with permission of Elsevier and Copyright Clearance Center.

MO dye removal from waters can be performed also by using simultaneously two different approaches: adsorption and catalysis. In their work, Liu and co-workers [84] studied the removal capacity of the organic-inorganic PGO-TiO_2/Fe_3O_4 (PGTF) hybrid material. The novel compound, prepared by loading TiO_2 and Fe_3O_4 onto polymeric ionic liquid (PIL) functionalized graphene oxide (GO), reached a removal rate of MO of about 95%. According to their conclusions, the excellent adsorption performance was due to the reticular structure of GO and to the presence of imidazole and $–NH_2$ in PIL. Additionally, the presence of imidazole cations in PIL have effectively promoted the separation of photogenerated electron–hole pairs and they enhanced the migration of photoexcited electrons, thereby increasing the photocatalytic efficiency.

Recently, heterogeneous semiconductor photocatalytic technology was widely adopted in environmental remediation and leveraging renewable solar energy to eliminate persistent organic pollutants from wastewater. For an effective photocatalysis, it is crucial to have photocatalysts that can efficiently capture visible light and facilitate the rapid separation of photoelectron–hole pairs, enabling thus the effective degradation of pollutants.

In recent years, researchers found that Ag^0/AgX (X = Cl, Br) composites own notable photocatalytic properties. However, the challenge of recycling in a heterogeneous phase reaction system is intensified by the small particle size and non-magnetic nature of nanocomposite photocatalysts. A straightforward solution to this problem is to integrate photocatalysts with magnetic materials and to use magnetic separation techniques. This solution was employed by Zhang and co-workers [85] for the preparation of Ag@AgBr/CN/Fe_3O_4 heterojunction photocatalysts, which are able to efficiently remove Rhodamine B (RhB) from wastewaters (Figure 10).

The study revealed that the removal and mineralization rates of RhB reached 96% and 47%, respectively, for 5% Ag loading and 0.4 g/L catalyst dosage. The study of the reaction mechanism has shown that the enhancement of the photocatalytic activity is performed by the creation of a Z-scheme heterojunction between Ag@AgBr and CN, along

with trapping of electrons by Fe^{3+}, promoting thus the charge transfer and the separation of electron–hole pairs.

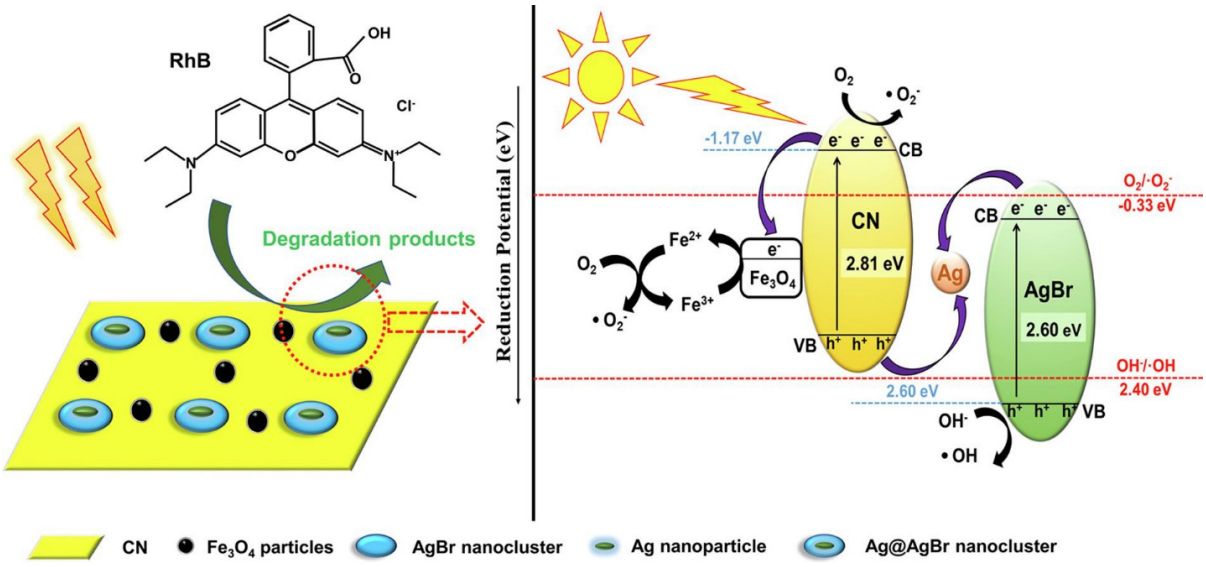


Figure 10. Degradation of RhB by Ag@AgBr/CN/Fe_3O_4 heterojunction photocatalysts. Source [85] with permission of Elsevier and Copyright Clearance Center.

The degradation of RhB dye in wastewater was studied by Han and co-workers [86] by photo-Fenton-like catalytic degradation of RhB. In their research, the authors have developed a new class of catalytic materials based on three dimensional self-assembled structures of MoS_2/Fe_3O_4 nanocomposites. The magnetic nanocomposite catalysts were prepared by hydrothermal route starting from Fe_3O_4 magnetite nanoparticles and MoS_2 molybdenum disulfide microspheres. After preparation, the nanocomposite materials were used for RhB degradation. The obtained results showed that the as-synthesized MoS_2/Fe_3O_4 nanocomposites manifest excellent photo-Fenton-like catalytic performances for the removal of RhB dyes from wastewater.

Another composite material, developed by Li and collaborators [87], able to efficiently decompose RhB by photocatalytic reaction is Fe_3O_4@TiO_2. The composite synthesis consists of two steps: in the first step, the TiO_2 nanoparticles are prepared, while in they are mixed with Fe_3O_4 the second step in order to cover the magnetic material surface to fabricate the Fe_3O_4@TiO_2 composite material. For the preparation of the TiO_2 nanoparticles$TiO(OH)_2$ is dissolved in concentrated H_2SO_4, in the first step while in the second step the Ti^{4+} ions are precipitated as $Ti(OH)_4$ by addition of ammonia solution. Afterwords, the precipitate is calcined at 550 °C for 2.5 h, in order to obtain the TiO_2 nanoparticles. Once the nanoparticles are prepared, they are mixed with a solution of functionalized Fe_3O_4 particles and, after 30 min of stirring, the final compound is collected by magnetic separation. During the degradation test, the material has demonstrated effective photocatalytic degradation of RhB along with slight recovery of the catalyst composite material, due to the presence of magnetite particles.

Based on core–shell Fe_3O_4@SiO_2 and rCu_2O-rGO, Liu and collaborators have developed a new class of photocatalytic composite materials, i.e rhombic dodecahedral cuprous oxide-reduced graphene oxide/core–shell Fe_3O_4@SiO_2 composites (rCu2O-rGO/Fe_3O_4@SiO_2) [88]. The composite material, prepared by the wet-chemical method, was used for the treatment of waters polluted with MO. The study revealed that the rCu_2O-rGO/Fe_3O_4@SiO_2 nanocomposite exhibited superior photocatalytic performance for MO degradation under visible light. Using only a 0.125 g L^{-1} photocatalyst concentration, almost 100% pollutant photodegradation was achieved within 60 min of irradiation. The remarkable catalytic performance may have resulted from the special interfacial interactions of rhombic dodec-

ahedra Cu_2O nanoparticles with the surface of rGO nanosheets, facilitating the electron release and transport along with the MO adsorption, contributing thus to the increase in the catalytic performance of the composite material.

The degradation of MB by Fenton oxidation was studied also by Ayadi and collaborators [89]. Ayadi et al. used magnetite decorated montmorillonite catalyst (Fe_3O_4/MMT) as composite materials. The material, prepared by the co-precipitation method, adsorbed the MB, while the Fe_3O_4 nanoparticles (which are predominantly located on the MMT surface) acted as catalysts for the MB degradation.

2.2.2. Phenolic Compounds Removal

Due to the low toxicity of the iron oxide nanoparticles and the environmentally friendly, Fe-based nanoparticles were studied as possible catalysts for other pollutants, such as phenolic compounds. The catalytic activity of magnetite-based composite nanoparticles for phenol degradation was studied by Gao and collaborators [90]. In their study, the efficiency of Fe_2O_3-ZrO_2 catalyst for phenol degradation by Fenton-like reaction was investigated. The materials were prepared by the sol–gel method. The yellow gel was obtained by thermal treatment at 80 °C for 5 h, and citric acid was added in an aqueous solution of $Fe(NO_3)_3 \cdot 9H_2O$ and $Zr(NO_3)_4 \cdot 5H_2O$. Besides the fact that Fe_2O_3-ZrO_2 catalyst can be easily separated from the reaction media, the obtained results show that this catalyst exhibited good phenol removal. Based on these results, Gao et al. [90] concluded that the Fe_2O_3-ZrO_2 catalyst could be successfully used for the wastewater treatment.

The physico-chemical properties of iron-based nanoparticles make these compounds suitable for use as catalysts for applications such as bisphenol A (BPA) catalytic degradation. Chen and co-workers [91] have prepared Fe/Fe_3O_4 composites embedded in N-doped graphite-like carbon nanosheets with entangled carbon nanotubes (CNTs) by one-step pyrolysis synthesis method and using $Fe(NO_3)_3 \cdot 9H_2O$, D-Alanine, and melamine. The composite material was tested as a catalyst for BPA degradation, with the results showing a high degradation efficiency of BPA. Moreover, the nanocomposite compound exhibited good cycle stability and a low Fe leaching rate, along with the fact that it can be easily recovered from the reaction solution due to the magnetic character. The removal of BPA from wastewaters was also studied by Cui and co-workers [92]. In their work, the authors have compared the catalytic activity of simple Fe_3O_4 nanoparticles with that of nano-Fe_3O_4-biochar (Fe_3O_4-BC) heterogeneous catalysts prepared by co-precipitation methods [92]. The results of [92] showed that the Fe_3O_4-BC system is a better catalyst than Fe_3O_4, the Fe_3O_4-BC system, removing the BPA more efficiently in an acidic medium. The authors found that the removal efficiency of the BPA after 90 min contact time is 100% for Fe_3O_4-BC while that of the Fe_3O_4 is 54.77%. The conclusion of the study was that the increase in the removal efficiency is due to the synergistic effect between Fe_3O_4 and BC.

Due to the toxicity of the 4-NP compound, its removal from the environment is necessary. The catalytic reduction of 4-NP to 4-aminophenol (4-AP) by using $NaBH_4$ as reduction agent is the most commonly used technique. This technique involves the use of catalysts with the role of facilitating the production of the chemical reaction. Among the most widely used catalysts are the noble metals [93–95]. However, the high price of the noble metals along with their scarcity led to the need to reduce the amount of noble metal used as a catalyst preserving, at the same time, the efficiency of the catalytic reaction [96].

One of the methods used by researchers to avoid the utilization of high quantities of noble metals is to decrease the size of catalysts, using simple or core–shell nanoparticles. Thus, Hu and collaborators [97] have loaded Au NPs onto the surface of metal–organic frameworks MOFs (NH_2-MIL-101(Fe)) to prepare Au@NH_2-MIL-101(Fe) nanocomposites. The new material was used as a catalyst for 4-NP reduction (Figure 11). The results showed that the Au@NH_2-MIL-101(Fe) nanocomposite manifested high catalytic performance and good recyclability, at the same time being easy to separate from the reaction environment by magnetic separation.

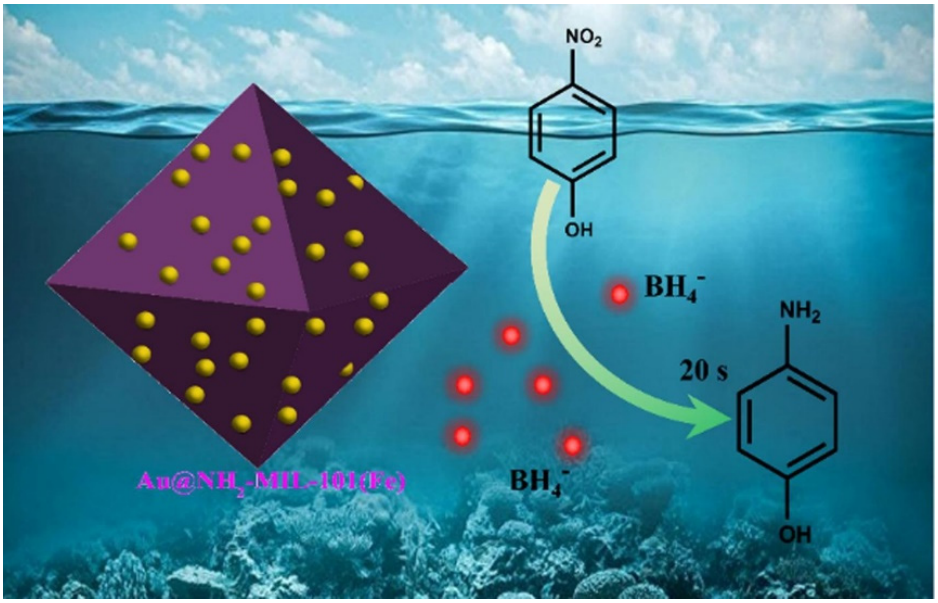


Figure 11. Graphic representation of the 4-NP reduction in presence of $NaBH_4$. Source [97] with permission from Elsevier and Copyright Clearance Center.

Another class of materials with excellent performance and recyclability for the photocatalytic removal of phenol, at the same time being magnetically separable, is represented by nanocomposites made of visible active N-doped TiO_2 based on SiO_2/Fe_3O_4 ferromagnetic nanoparticles (N-TiO_2/FM) [98]. The study revealed that the N-TiO_2/FM composite can reach a phenol degradation and total organic carbon (TOC) removal of 64% and 55%, respectively, after 270 min irradiation time.

One of the removal methods of the 2,4,6-trichlorophenol (TCP) from wastewaters is the photocatalytic oxidation on non-magnetic catalysts such as TiO_2 [99], ZnO [100–102], polymers [103], Ag/TiO_2 nanotube [104] or on magnetic catalysts such as lanthanum doped magnetic TiO_2 (Fe_3O_4/SiO_2/La-TiO_2) [105], Ag^0/Fe_3O_4 nanocomposite [106], Fe_3O_4@TiO_2@Au core–shell microspheres [107], CeO_2/Fe_3O_4 [108] or Fe_3O_4/CeO_2 composite [109]. The addition of magnetite in the composition of the catalyst leads not only to the increase in its efficiency but also to its reuse, the catalyst being easily separated from the reaction medium with the help of a magnet. The degradation of TCP by a heterogeneous Fenton-like system, using magnetic nanoscaled Fe_3O_4/CeO_2 composites, showed a higher removal rate of TCP as compared to others catalyst materials. Working at a solution pH 2.0 and by using 2.5 g/L Fe_3O_4/CeO_2 catalyst concentration the removal efficiency, mineralization, and dechlorination rate of TCP were 99%, 65% and 95% after 90 min, respectively [109].

A novel approach for creating stable, highly effective non-noble metal catalysts, developed by researchers in the recent years, assumed the combination of metal oxide nanoparticles (NPs) catalyst with electron carriers such as CNTs. By using this approach, Liu and collaborators have prepared, using the chemical vapor deposition technique, Fe_3O_4@CNT composite materials and have tested them as catalysts for the degradation of tetracycline [110]. The role of the CNTs is not only to accelerate electrons transfer and to prevent nanoparticles agglomeration, but also to avoid the Fe_3O_4 NPs oxidation in the reaction environment, increasing at the same time the composite catalytic activity. The as prepared composite material displayed a high removal efficiency of tetracycline from polluted water (89.1%), proving thus that it can be successfully used in water remediation.

2.2.3. Simultaneous Removal of High-Risk Contaminants

From a practical point of view, it is difficult to prepare filters for remediation of water containing various types of pollutants, by using materials specialized to remove a particular pollutant so that the development of advanced multifunctional materials

able to remove different classes of pollutants is necessary. Taking into account these new requirements, but also the fact that industrial development has led to water pollution with new and diverse pollutants, Mao and collaborators developed a multifunctional material for water purification based on mesoporous g-C_3N_4, nanosized Fe_3O_4, and aminopropyl triethoxysilane [111]. This material can be used for the remediation of water polluted with Cu(II) ions (by adsorption) and with organic pollutants such as RhB, phenol, and BPA (removed by photocatalytic degradation). The organic compounds degradation rate and efficiency of the MPG-C_3N_4/Fe_3O_4/NH_2 material reached 95% within 40 min, being able to use the composite with high efficiency for organic compounds degradation by the photoactivated Fenton reaction, even for five cycles.

Based on graphite carbon nitride (g-C_3N_4, GCN), Moradi and co-workers [112] prepared a new multifunctional composite catalyst by coupling g-C_3N_4 with spinel cobalt ferrite (SCF) nanoparticles. The as-prepared material was tested for remediation of water polluted with organic compounds, more specifically with BPA. The results showed that, through the SCF@GCN/PS/UVC system, photocatalytic and PS-based oxidation processes were both used to degrade the BPA. The authors concluded that the photodegradation of BPA on SCFO@GCN can be reasonably explained by a S-scheme heterojunction mechanism (Figure 12a). This mechanism is consistent with the scavenger tests and suggests a significant reduction in the recombination of electron–hole pairs through interfacial charge transfer, in alignement with the PL analysis results. Figure 12b, depicts the proposed mechanism of UVC-assisted activation of PS by SCFO@GCN under the S-scheme heterojunction mechanism. As shown, photogenerated electrons in the conduction band of GCN can activate PS molecules, producing SO_4• radicals, which enhance the oxidative degradation of BPA.

Dadashi and collaborators [113] developed a new class of multifunctional materials able to remove efficiently the Cr(VI), the 4-nitrophenol (4-NP),and organic dyes such as CR and MB from the aqueous media. The material was prepared by immobilization of copper (II) over the Fe_3O_4@SiO_2 nanoparticles (NPs) surface [Fe_3O_4@SiO_2-L–Cu(II)] (L = pyridine-4-carbaldehyde thiosemicarbazide). The obtained results have demonstrated that the new catalyst material could be easily separated and maintained 83% of its efficiency, after five cycles.

An efficient and multifunctional nanocomposite material, able to catalyticallly reduce various organic water pollutants (such as 4-NP, MB, CR, MO and RhB), based on alkyl-functionalized Fe_3O_4 magnetite core and a layered chitosan (CTS) shell loaded with Au nanoparticles, was synthesized by Hu and collaborators [114]. The newly prepared Fe_3O_4@C16@CTS-Au nanocomposite material manifests high catalytic efficiency and stability over similar catalysts, being easily separable from the reaction environment. Even after being recycled eleven times or kept in storage for longer than a month, the catalyst good activity is maintained.

Wastewater polluted with a mixture of five different pollutant dyes (MO, metanil yellow—MY, CR, MB, crystal violet—CV), was successfully treated by Kaushik and coworkers [115] using reduced iron oxide dust (r-IOD, Fe_3O_4@α-Fe_2O_3), catalysts, and photodegradation processes in the presence of sunlight. Oxide dust (IOD), also known as Hematite (α-Fe_2O_3), is a steel industries waste product generated in tons. After characterization, the synthesized magnetic r-IOD was used to degrade complex cationic and anionic organic dyes from wastewater and soil samples. It was found that the anionic dyes were completely removed, i.e., 94.1%, 94.4%, and 93.3% for MO, MY, and CR, respectively while the removal was partial for the cationic dyes (i.e., 35.5% and 68.8% in case of MB and CV, respectively).

The simultaneous removal of CR dyes and heavy metal ions was studied by Lu and collaborators [116]. A new N, S-CQDs@Fe_3O_4@HTC composite was prepared by the authors by loading N, S carbon quantum dots (N, S-CQDs), derived from lignin, on magnetic hydrotalcite (HTC). The new N, S-CQDs@Fe_3O_4@HTC composite had excellent stability and recyclability during five cycles, showing good UV degradation of CR, with

efficiencies over 95.43%, as well as good efficiency for simultaneously removal of Cu(II) (99.90%) and Cd(II) (85.08%).

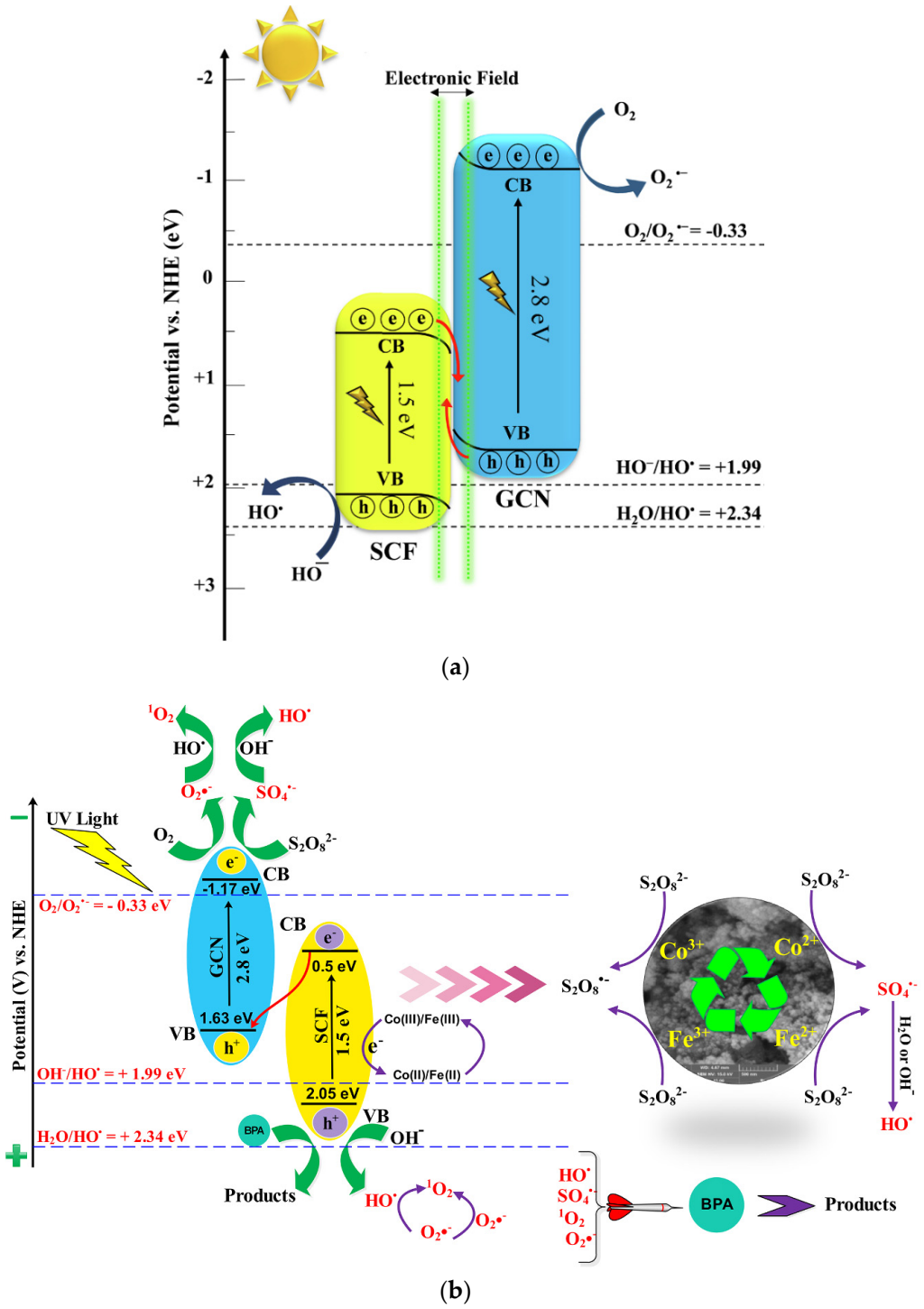


Figure 12. Proposition for the photocatalytic mechanism of SCF@GCN (**a**) and the possible UVC-assisted activation of PS by SCF@GCN under the S-scheme heterojunction mechanism (**b**). Source [112] with permission of Elsevier and Copyright Clearance Center.

3. Conclusions

In the present paper, we reviewed the capacity of magnetic composite materials, based on LDH and Fe_3O_4, to remove different categories of pollutants from wastewaters using the adsorption process. The ability of various types of magnetic compounds as catalysts for

water treatment is discussed as well. One of the main advantages presented by magnetic composite materials is the ease of separation from solution.

The main findings, after reviewing the literature, are presented below:

- The critical water pollutants, specifically heavy metals, dyes, pharmaceutical products, phenolic compounds, phytohormone, and fungicides can be successfully removed by using both the adsorption and/or catalytic processes.
- Based on the reviewed papers, where results have been presented for real waters and, mostly, for synthetically prepared wastewaters, it can be concluded that the magnetic composite materials based on LDH and Fe_3O_4 may be considered as efficient adsorbents, especially for heavy metals and dye removal.
- Although the wastewaters contaminated with phenolic compounds are frequently treated by using the catalytic processes, the studies have demonstrated that the adsorption method is a good alternative.
- The ability of composite magnetic materials for the elimination of other categories of pollutants, specifically for the removal of some antibiotics and fungicides, was also reviewed. The results demonstrated that these types of composite magnetic materials can be successfully applied in water depollution.
- The removal of dyes from polluted waters, using catalytic degradation, can be achieved with high efficiency (higher than 98%) using composite magnetic materials based on magnetite TiO_2, SiO_2, CeO_2, MoS_2 as catalysts but also using hybrid materials containing an organic compound as well as magnetite (such as PGO-TiO_2/Fe_3O_4, Ag@AgBr/CN/Fe_3O_4, rCu_2O-rGO/Fe_3O_4@SiO_2, Fe_3O_4/MMT).
- The catalytic degradation of phenols from wastewaters can achieve 100% efficiency by using Fe_3O_4-BC heterogeneous catalysts. The increase in the catalytic efficiency from 54.77% (when Fe_3O_4 is used as catalyst) to 100% (when Fe_3O_4 –BC is used as catalyst) is due to the synergistic effect between the Fe_3O_4 nanoparticles and the biochar.
- The second approach used for the treatment of wastewaters polluted with phenols (more precisely nitrophenols), is the catalytic reduction of the nitro group in the amino group. The magnetic nanocomposite materials can be successfully used as catalysts for performing the chemical reduction in presence of $NaBH_4$.
- Pharmaceutical products can also be eliminated from polluted waters by catalytic degradation, the reaction being able to reach an efficiency as high as 89.1%.
- Several authors have shown that catalytic degradation is efficient also for purifying waters polluted with multiple pollutants. Thus, multifunctional materials have been developed in order to efficiently clean waters polluted with dyes and phenols, heavy metals, or dyes and nitrophenols.

The studies reviewed in this article are based on the literature that refer to the use of these materials for wastewater treatment at the laboratory scale. Future review should focus on the application of these types of composite magnetic materials at the pilot scale. Special attention should be paid to the treatment of real wastewaters.

Author Contributions: Conceptualization, O.-G.D.-P. and G.B.; investigation, O.-G.D.-P. and G.B.; writing—original draft preparation, O.-G.D.-P. and G.B.; writing—review and editing, N.L. and H.C.; project administration, O.-G.D.-P. and N.L.; funding acquisition, O.-G.D.-P. and N.L. All authors have read and agreed to the published version of the manuscript.

Funding: This study was supported by a grant of the Ministry of Research, Innovation and Digitization under the Nucleu-program within the National Research Development and Innovation Plan 2022-2027, Project number PN 23 11 01 01. This work was supported by a grant of the Ministry of Research, Innovation and Digitalization, CNCS-UEFISCDI, project number PN-III-P4-PCE-2021-1395/GreenEn, within PNCDI III.

Conflicts of Interest: The authors declare no conflicts of interest.

References

1. Abin-Bazaine, A.; Campos Trujillo, A.; Olmos-Marquez, M. Adsorption Isotherms: Enlightenment of the Phenomenon of Adsorption. In *Wastewater Treatment*; IntechOpen: London, UK, 2022. [CrossRef]
2. William Kajjumba, G.; Emik, S.; Öngen, A.; Kurtulus Özcan, H.; Aydın, S. Modelling of Adsorption Kinetic Processes—Errors, Theory and Application. In *Advanced Sorption Process Applications*; IntechOpen: London, UK, 2019. [CrossRef]
3. Mustapha, S.; Shuaib, D.T.; Ndamitso, M.M.; Etsuyankpa, M.B.; Sumaila, A.; Mohammed, U.M.; Nasirudeen, M.B. Adsorption isotherm, kinetic and thermodynamic studies for the removal of Pb(II), Cd(II), Zn(II) and Cu(II) ions from aqueous solutions using Albizia lebbeck pods. *Appl. Water Sci.* **2019**, *9*, 142. [CrossRef]
4. Batool, F.; Akbar, J.; Iqbal, S.; Noreen, S.; Bukhari, S.N.A. Study of Isothermal, Kinetic, and Thermodynamic Parameters for Adsorption of Cadmium: An Overview of Linear and Nonlinear Approach and Error Analysis. *Bioinorg. Chem. Appl.* **2018**, *2018*, 3463724. [CrossRef]
5. Raghuwanshi, M.; Singh, A.; Suryawanshi, B.; Yash Jaiswal, Y. Synthesis and characterization of MgAl- layered double hydroxide with graphene oxide intercalation: Application in lead removal from spent batteries effluent. *Mater. Today Proc.* **2024**, *in press*. [CrossRef]
6. Johnston, A.L.; Lester, E.; Williams, O.; Gomes, R.L. Understanding Layered Double Hydroxide properties as sorbent materials for removing organic pollutants from environmental waters. *J. Environ. Chem. Eng.* **2021**, *9*, 105197. [CrossRef]
7. Cheng, J.; Liang, C.; Lin, W.; Zeng, J.; Li, C.; Li, S.; Zhang, F.; Wang, Y. Preparation and characterization of phase change material microcapsules with carbon nanotubes loaded with MgAl layered double hydroxides for controlling temperature in the building. *J. Energy Storage* **2024**, *80*, 110357. [CrossRef]
8. Maegawa, K.; Zhang, F.; Johnson, Q.; Jitianu, M.; Tan, W.K.; Kawamura, G.; Matsuda, A.; Jitianu, A. Control of Micro- and Nanostructures of Layered Double Hydroxides by Hydrothermal Treatment. *Cryst. Growth Des.* **2023**, *23*, 2128–2137. [CrossRef]
9. Takanashi, I.; Kameda, T.; Kumagai, S.; Saito, Y.; Nomura, Y.; Kawamura, D.; Yoshioka, T. Synthesis of layered double oxide with high specific surface area by innovative sol-gel method through its application to arsenate anion adsorption. *J. Alloys Compd.* **2023**, *960*, 170865. [CrossRef]
10. Khomeyrani, S.F.N.; Ghalami-Choobar, B.; Azqhandi, M.H.A.; Foroughi, M. An enhanced removal of para-nitrophenol (PNP) from water media using CaAl-layered double hydroxide-loaded magnetic g-CN nanocomposite. *J. Water Process Eng.* **2022**, *46*, 102516. [CrossRef]
11. Knorpp, A.J.; Zawisza, A.; Huangfu, S.; Borzì, A.; Clark, A.H.; Kata, D.; Graule, T.; Stuer, M. Hydrothermal synthesis of multi-cationic high-entropy layered double hydroxides. *RCS Adv.* **2022**, *12*, 26362–26371. [CrossRef]
12. Tung, N.Q.; Van, D.C.; Thang, D.X.; An, N.T.K.; Trang, T.T.; Nhi, B.D.; Thao, N.P.; Son, L.; Huy, N.N.; Dung, N.T. Hydrothermal synthesis of CuCoFe layered double hydroxide and its performance in the degradation of antibiotics: Influencing factors, degradation pathways, and reaction mechanism. *J. Environ. Chem. Eng.* **2023**, *11*, 110127. [CrossRef]
13. Bukhtiyarova, M.V. A review on effect of synthesis conditions on the formation of layered double hydroxide. *J. Solid State Chem.* **2019**, *269*, 494–506. [CrossRef]
14. Feng, X.; Long, R.; Wang, L.; Liu, C.; Bai, Z.; Liu, X. A review on heavy metal ions adsorption from water by layered double hydroxide and its composites. *Sep. Purif. Technol.* **2022**, *284*, 120099. [CrossRef]
15. Cano, L.A.; Barrera, D.; Villarroel-Rocha, J.; Sapag, K. Influence of the synthesis method of layered double hydroxides on the textural properties and nitrate removal. *Catal. Today* **2023**, *422*, 114222. [CrossRef]
16. Tichit, D.; Layrac, G.; Alvarez, M.G.; Marcu, I.C. Formation pathways of MII/MIII layered double hydroxides: A review. *Appl. Clay Sci.* **2024**, *248*, 107234. [CrossRef]
17. Chaillot, D.; Bennici, S.; Brendlé, J. Layered double hydroxides and LDH-derived materials in chosen environmental applications: A review. *Environ. Sci. Pollut. Res.* **2021**, *28*, 24375–24405. [CrossRef] [PubMed]
18. Molaei, M.J. Magnetic two-dimensional Ca-Al layered double hydroxide/Fe_3O_4@dextran nanocomposites as drug delivery systems. *J. Cryst. Growth* **2023**, *611*, 127186. [CrossRef]
19. Zheng, T.; Wu, H.; Han, Z.; Chen, L.; Tang, B.; Cui, P.; Liu, H.; Chao, Y.; Zhu, W.; Liu, Z. Boron nitride modified CuZn-calcinated layered double hydroxides as efficient adsorbents for tetracycline removal. *Sep. Purif. Technol.* **2024**, *340*, 126648. [CrossRef]
20. Dudchenko, N.; Pawar, S.; Perelshtein, I.; Fixler, D. Magnetite Nanoparticles: Synthesis and Applications in Optics and Nanophotonics. *Materials* **2022**, *15*, 2601. [CrossRef]
21. Loiola, A.R.; Bessa, R.A.; Oliveira, C.P.; Freitas, A.D.L.; Soares, S.A.; Bohn, F.; Pergher, S.B.C. Magnetic zeolite composites: Classification, synthesis routes, and technological applications. *J. Magn. Magn. Mater.* **2022**, *560*, 169651. [CrossRef]
22. Zhang, J.; Lin, S.; Han, M.; Su, Q.; Xia, L.; Hui, Z. Adsorption Properties of Magnetic Magnetite Nanoparticle for Coexistent Cr(VI) and Cu(II) in Mixed Solution. *Water* **2020**, *12*, 446. [CrossRef]
23. Hudcová, B.; Veselská, V.; Filip, J.; Číhalová, S.; Komárek, M. Highly effective Zn(II) and Pb(II) removal from aqueous solutions using Mg-Fe layered double hydroxides: Comprehensive adsorption modeling coupled with solid state analyses. *J. Clean. Prod.* **2018**, *171*, 944–953. [CrossRef]
24. Tran, H.N.; Lin, C.C.; Woo, S.H.; Huang-Ping Chao, H.P. Efficient removal of copper and lead by Mg/Al layered double hydroxides intercalated with organic acid anions: Adsorption kinetics, isotherms, and thermodynamics. *Appl. Clay Sci.* **2018**, *154*, 17–27. [CrossRef]

25. Dalla Nora, F.B.; Lima, V.V.C.; Oliveira, M.L.S.; Hosseini-Bandegharaei, A.; Lima Burgo, T.A.; Meili, L.; Dotto, G.L. Adsorptive potential of Zn–Al and Mg–Fe layered double hydroxides for the removal of 2–nitrophenol from aqueous solutions. *J. Environ. Chem. Eng.* **2020**, *8*, 103913. [CrossRef]
26. Awes, H.; Zaki, Z.; Abbas, S.; Dessoukii, H.; Zaher, A.; Abd-El Moaty, S.A.; Shehata, N.; Farghali, A.; Mahmoud, R.K. Removal of Cu^{2+} metal ions from water using Mg-Fe layered double hydroxide and Mg-Fe LDH/5-(3-nitrophenyllazo)-6-aminouracil nanocomposite for enhancing adsorption properties. *Environ. Sci. Pollut. Res.* **2021**, *28*, 47651–47667. [CrossRef]
27. Abdel-Hady, E.E.; Mohamed, H.F.M.; Hafez, S.H.M.; Fahmy, A.M.M.; Magdy, A.; Mohamed, A.S.; Ali, E.O.; Abdelhamed, H.R.; Mahmoud, O.M. Textural properties and adsorption behavior of Zn-Mg-Al layered double hydroxide upon crystal violet dye removal as a low cost, effective, and recyclable adsorbent. *Sci. Rep.* **2023**, *13*, 6435. [CrossRef] [PubMed]
28. Alghamdi, A.G.; Ahmad, J.; Alasmari, Z.; Ibrahim, H.M. Removal of hexavalent chromium from contaminated soil and water by Mg/Fe layered double hydroxide and its composite with biochar. *Arab. J. Geosci.* **2023**, *16*, 145. [CrossRef]
29. Iconaru, S.L.; Guégan, R.; Popa, C.L.; Motelica-Heino, M.; Ciobanu, C.S.; Daniela Predoi, D. Magnetite (Fe_3O_4) nanoparticles as adsorbents for As and Cu removal. *Appl. Clay Sci.* **2016**, *134*, 128–135. [CrossRef]
30. Prasad, C.; Tang, H.; Liu, W. Magnetic Fe_3O_4 based layered double hydroxides (LDHs) nanocomposites (Fe_3O_4/LDHs): Recent review of progress in synthesis, properties and applications. *J. Nanostruct. Chem.* **2018**, *8*, 393–412. [CrossRef]
31. Sun, J.H.; Chen, Y.; Yu, H.Q.; Yan, L.G.; Du, B.; Pei, Z.G. Removal of Cu^{2+}, Cd^{2+} and Pb^{2+} from aqueous solutions by magnetic alginate microsphere based on Fe_3O_4/MgAl-layered double hydroxide. *J. Colloid Interface Sci.* **2018**, *532*, 474–484. [CrossRef]
32. Hou, T.; Yan, L.; Li, J.; Yang, Y.; Shan, L.; Meng, X.; Li, X.; Zhao, Y. Adsorption performance and mechanistic study of heavy metals by facile synthesized magnetic layered double oxide/carbon composite from spent adsorbent. *Chem. Eng. J.* **2020**, *384*, 123331. [CrossRef]
33. Behbahani, E.S.; Dashtian, K.; Ghaedi, M. Fe_3O_4-$FeMoS_4$: Promise magnetite LDH-based adsorbent for simultaneous removal of Pb (II), Cd (II), and Cu (II) heavy metal ions. *J. Hazard. Mater.* **2021**, *410*, 124560. [CrossRef] [PubMed]
34. Gherca, D.; Borhan, A.I.; Mihai, M.M.; Herea, D.D.; Stoian, G.; Roman, T.; Chiriac, H.; Lupu, N.; Buema, G. Magnetite-induced topological transformation of 3D hierarchical MgAl layered double hydroxides to highly dispersed 2D magnetic hetero-nanosheets for effective removal of cadmium ions from aqueous solutions. *Mater. Chem. Phys.* **2022**, *284*, 126047. [CrossRef]
35. Li, Y.; Bi, H.Y.; Liang, Y.Q.; Mao, X.M.; Li, H. Synthesis of novel magnetic rhamnolipid-activated layered double hydroxides nanocomposite for simultaneous adsorption of Cu(II) and m-cresol from aqueous solution. *Powder Technol.* **2021**, *386*, 350–360. [CrossRef]
36. Taheri, S.; Sedghi-Asl, M.; Ghaedi, M.; Mohammadi-Asl, Z.; Rahmanian, M. Magnetic layered double hydroxide composite as new adsorbent for efficient Cu (II) and Ni (II) ions removal from aqueous samples: Adsorption mechanism investigation and parameters optimization. *J. Environ. Manag.* **2023**, *329*, 117009. [CrossRef] [PubMed]
37. Xie, Y.Y.; Yuan, X.Z.; Wu, Z.B.; Zeng, G.M.; Jiang, L.B.; Peng, X.; Li, H. Adsorption behavior and mechanism of Mg/Fe layered double hydroxide with Fe_3O_4-carbon spheres on the removal of Pb(II) and Cu(II). *J. Colloid Interface Sci.* **2019**, *536*, 440–455. [CrossRef] [PubMed]
38. Zhang, H.; Huang, F.; Liu, D.L.; Shi, P. Highly efficient removal of Cr(VI) from wastewater via adsorption with novel magnetic Fe_3O_4@C@MgAl-layered double-hydroxide. *Chin. Chem. Lett.* **2015**, *26*, 1137–1143. [CrossRef]
39. Sun, G.; Zhang, J.; Li, X.; Hao, B.; Xu, F.; Liu, K. Self-assembled morphology-controlled hierarchical Fe_3O_4@LDH for Cr(VI) removal. *J. Environ. Chem. Eng.* **2023**, *11*, 110129. [CrossRef]
40. Hong, X.; Ding, C.; Shi, M.; Ding, Z.; Du, P.; Xia, M.; Wang, F. Easy separation dual-function Cu_2O@LDH@Fe_3O_4 adsorbent for the removal of Cr(VI) under dark conditions: Experimental and mechanistic study. *Sep. Purif. Technol.* **2024**, *332*, 125734. [CrossRef]
41. Zhao, S.F.; Wu, M.; Jing, R.S.; Liu, X.J.; Shao, Y.F.; Zhang, Q.; Lv, F.Z.; Liu, A.J.; Meng, Z.L. One-pot formation of magnetic layered double hydroxide based on electrostatic self-assembly to remove Cr(VI) from wastewater. *Appl. Clay Sci.* **2019**, *182*, 105297. [CrossRef]
42. Dinari, M.; Shirani, M.A.; Maleki, M.H.; Tabatabaeian, R. Green cross-linked bionanocomposite of magnetic layered double hydroxide/guar gum polymer as an efficient adsorbent of Cr(VI) from aqueous solution. *Carbohydr. Polym.* **2020**, *236*, 116070. [CrossRef]
43. Kobylinska, N.; Puzyrnaya, L.; Pshinko, G. Magnetic nanocomposites based on Zn,Al-LDH intercalated with citric and EDTA groups for the removal of U(vi) from environmental and wastewater: Synergistic effect and adsorption mechanism study. *RCS Adv.* **2022**, *12*, 32156–32172. [CrossRef] [PubMed]
44. Shou, J.X.; Jiang, C.F.; Wang, F.; Qiu, M.Q.; Xu, Q.G. Fabrication of Fe_3O_4/MgAl-layered double hydroxide magnetic composites for the effective decontamination of Co(II) from synthetic wastewater. *J. Mol. Liq.* **2015**, *207*, 216–223. [CrossRef]
45. Lu, L.; Li, J.; Ng, D.H.L.; Yang, P.; Song, P.; Zuo, M. Synthesis of novel hierarchically porous Fe_3O_4@MgAl–LDH magnetic microspheres and its superb adsorption properties of dye from water. *J. Ind. Eng. Chem.* **2017**, *46*, 315–323. [CrossRef]
46. Wu, X.G.; Li, B.; Wen, X.G. Synthesis and adsorption properties of hierarchical Fe_3O_4@MgAl-LDH magnetic microspheres. *J. Nanopart. Res.* **2017**, *19*, 131. [CrossRef]
47. Chengqian, F.; Yimin, D.; Ling, C.; Zhiheng, W.; Qi, L.; Yaqi, L.; Ling, C.; Bo, L.; Yue-Fei, Z.; Yan, L.; et al. One-step coprecipitation synthesis of Cl^- intercalated Fe_3O_4@SiO_2 @MgAl LDH nanocomposites with excellent adsorption performance toward three dyes. *Sep. Purif. Technol.* **2022**, *295*, 121227. [CrossRef]

48. Chengqian, F.; Wanbing, L.; Yimin, D.; Zhiheng, W.; Yaqi, L.; Ling, C.; Bo, L.; Siwen, Y.; Junlong, W.; Xianglong, D.; et al. Synthesis of a novel hierarchical pillared Sep@Fe_3O_4/ZnAl-LDH composite for effective anionic dyes removal. *Colloids Surf. A Physicochem. Eng. Asp.* **2023**, *663*, 130921. [CrossRef]
49. Mallakpour, S.; Hatami, M. An effective, low-cost and recyclable bio-adsorbent having amino acid intercalated LDH@Fe_3O_4/PVA magnetic nanocomposites for removal of methyl orange from aqueous solution. *Appl. Clay Sci.* **2019**, *174*, 127–137. [CrossRef]
50. Natarajan, S.; Anitha, V.; Gajula, G.P.; Thiagarajan, V. Synthesis and Characterization of Magnetic Superadsorbent Fe_3O_4-PEG-Mg-Al-LDH Nanocomposites for Ultrahigh Removal of Organic Dyes. *ACS Omega* **2020**, *5*, 3181–3193. [CrossRef]
51. Chen, D.; Li, Y.; Zhang, J.; Zhou, J.; Guo, Y.; Hong Liu, H. Magnetic Fe_3O_4/ZnCr-layered double hydroxide composite with enhanced adsorption and photocatalytic activity. *Chem. Eng. J.* **2012**, *185–186*, 120–126. [CrossRef]
52. Li, Y.; Bi, H.Y.; Liang, Y.Q.; Mao, X.M.; Li, H. A magnetic core-shell dodecyl sulfate intercalated layered double hydroxide nanocomposite for the adsorption of cationic and anionic organic dyes. *Appl. Clay Sci.* **2019**, *183*, 105309. [CrossRef]
53. Khooni, M.A.K.; Ahmadzadeh, H.; Davardoostmanesh, M. Magnetic graphene oxide/Mg-Al layered double hydroxide nanocomposite as an efficient adsorbent for removal of methylene blue: A study of equilibrium isotherms, kinetics, thermodynamic and reusability. *Mater. Sci. Eng. B* **2024**, *300*, 117123. [CrossRef]
54. Tabatabaeian, R.; Dinari, M.; Aliabadi, H.M. Cross-linked bionanocomposites of hydrolyzed guar gum/magnetic layered double hydroxide as an effective sorbent for methylene blue removal. *Carbohydr. Polym.* **2021**, *257*, 117628. [CrossRef] [PubMed]
55. Tang, Y.; Zhang, X.; Li, X.; Bai, J.; Yang, C.; Zhang, Y.; Xu, Z.; Jin, X.; Jiang, Y. Facile synthesis of magnetic ZnAl layered double hydroxides and efficient adsorption of malachite green and Congo red. *Sep. Purif. Technol.* **2023**, *322*, 124305. [CrossRef]
56. Liu, S.; Li, M.; Tang, Y.; Wen, X. A novel Fe_3O_4/MgAl-LDH hollow microspheres for effective removal of dyes from wastewater. *J. Alloys Compd.* **2023**, *959*, 170528. [CrossRef]
57. Ali, R.H.M.; Hsu, C.-Y.; Thalij, K.M.; Althomali, R.H.; Abdullaev, S.; Abdulameer, S.F.; Alawadi, A.H.; Alsaalamy, A.; Dawood, F.A.; Ahmed, N.M. An efficient magnetic nanoadsorbent based on functionalized graphene oxide with gellan gum hydrogel embedded with MnFe layered double hydroxide for adsorption of Indigo carmine from water. *Int. J. Biol. Macromol.* **2023**, *253*, 127479. [CrossRef] [PubMed]
58. Bagtash, M.; Zolgharnein, J. Carbon-Magnetic Layered Double Hydroxide as a New Nanosorbent for Efficient Removal of Tartrazine and Indigo Carmine Dyes from Water Solutions; Multivariate Optimization and Adsorption Characterization. *J. Water Chem. Technol.* **2022**, *44*, 259–268. [CrossRef]
59. Mohammadi, M.; Eivazzadeh-Keihan, R.; Babamoradi, M.; Ali Maleki, A. A magnetic and antibacterial nanocomposite based on graphene oxide nanosheets embedded with Zn-Fe layered double hydroxide as a novel and highly effective adsorbent for the removal of methylene blue dye. *Diam. Relat. Mater.* **2024**, *144*, 111010. [CrossRef]
60. Kheradmand, A.; Negarestani, M.; Kazemi, S.; Shayesteh, H.; Javanshir, S.; Ghiasinejad, H. Adsorption behavior of rhamnolipid modified magnetic Co/Al layered double hydroxide for the removal of cationic and anionic dyes. *Sci. Rep.* **2022**, *12*, 14623. [CrossRef]
61. Meira, A.C.R.; Zago, J.V.G.; Tremarin, B.G.; Mezalira, D.Z.; Cursino, A.C.T.; Bail, A.; Basso, R.L.D.; Giona, R.M. Enhancing adsorption capacity of magnetic magnesium-aluminum layered double hydroxide by surface modification with sodium dodecyl sulfate for efficient removal of organic contaminants. *J. Environ. Chem. Eng.* **2023**, *11*, 111443. [CrossRef]
62. Bagtash, M.; Zolgharnein, J. Response surface optimization for simultaneous removal of Alizarin Red S and Alizarin Yellow dyes from aqueous solution using magnetic Zn-Al-Zr layered double hydroxide. *Inorg. Nano-Met. Chem.* **2023**. [CrossRef]
63. Adlnasab, L.; Ezoddin, M.; Karimi, M.A.; Hatamikia, N. MCM-41@Cu-Fe-LDH magnetic nanoparticles modified with cationic surfactant for removal of Alizarin Yellow from water samples and its determination with HPLC. *Res. Chem. Intermed.* **2018**, *44*, 3249–3265. [CrossRef]
64. Gonçalves, R.G.L.; Lopes, P.A.; Resende, J.A.; Pinto, F.G.; Tronto, J.; Guerreiro, M.C.; de Oliveira, L.C.A.; Nunes, W.D.; Neto, J.L. Performance of magnetite/layered double hydroxide composite for dye removal via adsorption, Fenton and photo-Fenton processes. *Appl. Clay Sci.* **2019**, *179*, 105152. [CrossRef]
65. Zhang, D.; Zhu, M.Y.; Yu, J.G.; Meng, H.W.; Jiao, F.P. Effective removal of brilliant green from aqueous solution with magnetic Fe_3O_4@SDBS@LDHs composites. *Trans. Nonferr. Met. Soc. China* **2017**, *27*, 2673–2681. [CrossRef]
66. Yang, X.; Mao, L.; Shuai, H.; Rong, Q.; Zhang, S.; Lu, H. Ultrasound-assisted synthesis of magnetic layer CaAl hydrotalcite composite for removal of fuchsin acid in simulated solution. *Int. J. Environ. Sci. Technol.* **2024**, *21*, 1591–1604. [CrossRef]
67. Kheradmand, A.; Ghiasinejad, H.; Javanshir, S.; Khadir, A.; Jamshidi, E. Efficient removal of Ibuprofen via novel core—shell magnetic bio-surfactant rhamnolipid—layered double hydroxide nanocomposite. *J. Environ. Chem. Eng.* **2021**, *9*, 106158. [CrossRef]
68. Smata, A.; Yoshimura, C. One-step synthesis of magnetic–layered double hydroxide and its application for oxytetracycline removal from water. *J. Environ. Chem. Eng.* **2022**, *10*, 107819. [CrossRef]
69. Azqhandi, M.H.A.; Foroughi, M.; Gholami, Z. Efficient removal of levofloxacin by a magnetic NiFe-LDH/N-MWCNTs nanocomposite: Characterization, response surface methodology, and mechanism. *Environ. Res.* **2022**, *215*, 113967. [CrossRef]
70. Kheradmand, A.; Negarestani, M.; Kazemi, S.; Shayesteh, H.; Javanshir, S.; Ghiasinejad, H.; Jamshidi, E. Design and preparation magnetic bio-surfactant rhamnolipid-layered double hydroxide nanocomposite as an efficient and recyclable adsorbent for the removal of Rifampin from aqueous solution. *Sep. Purif. Technol.* **2023**, *304*, 122362. [CrossRef]

71. Wu, H.J.; Zhang, H.L.; Zhang, W.J.; Yang, X.F.; Zhou, H.; Pan, Z.Q.; Wang, D.S. Preparation of magnetic polyimide@ Mg-Fe layered double hydroxides core-shell composite for effective removal of various organic contaminants from aqueous solution. *Cremosphere* **2019**, *219*, 66–75. [CrossRef]
72. Fang, T.B.; Xiao, H.; Zhao, L.X.; Li, N.; Luan, L.Y.; Yan, Z.X.; Lin, J.M.; Zhao, R.S. Magnetic ternary layered double hydroxides for efficient removal of 1-naphthalene acetic acid from waters: Adsorption behavior and mechanism. *J. Environ. Chem. Eng.* **2023**, *11*, 109490. [CrossRef]
73. Zhao, L.X.; Xiao, H.; Li, M.H.; Xie, M.; Li, N.; Zhao, R.S. Effectively removing indole-3-butyric acid from aqueous solution with magnetic layered double hydroxide-based adsorbents. *J. Hazard. Mater.* **2021**, *408*, 124446. [CrossRef] [PubMed]
74. Lu, Z.H.; Senosy, I.A.; Zhou, D.D.; Yang, Z.H.; Guo, H.M.; Liu, X. Synthesis and adsorption properties investigation of Fe_3O_4@ZnAl-LDH@MIL-53(Al) for azole fungicides removal from environmental water. *Sep. Purif. Technol.* **2021**, *276*, 119282. [CrossRef]
75. Yasmina, M.; Mourad, K.; Mohammed, S.H.; Khaoula, C. Treatment heterogeneous photocatalysis. Factors influencing the photocatalytic degradation by TiO_2. *Energy Procedia* **2014**, *50*, 559–566. [CrossRef]
76. Atta, A.M.; Gafer, A.K.; Al-Lohedan, H.A.; Abdullah, M.M.S.; Tawfeek, A.M.; Ezzat, A.O. Hybrid Ionic Silver and Magnetite Microgels Nanocomposites for Efficient Removal of Methylene Blue. *Molecules* **2019**, *24*, 3867. [CrossRef] [PubMed]
77. Arora, P.; Fermah, A.; Rajput, J.K.; Singh, H.; Badhan, J. Efficient solar light-driven degradation of Congo red with novel Cu-loaded Fe_3O_4@TiO_2 nanoparticles. *Environ. Sci. Pollut. Res.* **2017**, *24*, 19546–19560. [CrossRef] [PubMed]
78. Zhu, L.; Kong, X.; Yang, C.; Ren, B.; Tang, Q. Fabrication and characterization of the magnetic separation photocatalyst C-TiO_2@Fe_3O_4/AC with enhanced photocatalytic performance under visible light irradiation. *J. Hazard. Mater.* **2020**, *381*, 120910. [CrossRef] [PubMed]
79. Eltaweil, A.S.; Bakr, S.S.; Abd El-Monaem, E.M.; El-Subruiti, G.M. Magnetic hierarchical flower-like Fe_3O_4@ZIF-67/CuNiMn-LDH catalyst with enhanced redox cycle for Fenton-like degradation of Congo red: Optimization and mechanism. *Environ. Sci. Pollut. Res.* **2023**, *30*, 75332–75348. [CrossRef] [PubMed]
80. Xiang, D.; Lu, S.; Ma, Y.; Zhao, L. Synergistic photocatalysis-fenton reaction of flower-shaped CeO_2/Fe_3O_4 magnetic catalyst for decolorization of high concentration congo red dye. *Colloids Surf. A Physicochem. Eng. Asp.* **2022**, *647*, 129021. [CrossRef]
81. Khan, A.U.; Salam, A.; Khan, H.; Qureshi, A.; Saeed, A. Green synthesis of magnetic chitosan composite hydrogel (Fe_3O_4@CS photocatalyst) for the solar light driven catalytic degradation of organic contaminants. *Anal. Chem. Lett.* **2024**, *14*, 112–128. [CrossRef]
82. Al-Abdallat, Y.; Jum'h, I.; Al Bsoul, A.; Jumah, R.; Telfah, A.; Telfah, A. Photocatalytic Degradation Dynamics of Methyl Orange Using Coprecipitation Synthesized Fe_3O_4 Nanoparticles. *Water Air Soil Pollut.* **2019**, *230*, 277. [CrossRef]
83. Arshad, A.; Iqbal, J.; Ahmad, I.; Israr, M. Graphene/Fe_3O_4 nanocomposite: Interplay between photo-Fenton type reaction, and carbon purity for the removal of methyl orange. *Ceram. Int.* **2018**, *44*, 2643–2648. [CrossRef]
84. Liu, H.; Wang, K.; Zhang, D.; Zhao, D.; Zhai, J.; Cui, W. Adsorption and catalytic removal of methyl orange from water by PIL-GO/TiO_2/Fe_3O_4 composites. *Mater. Sci. Semicond. Process.* **2023**, *154*, 107215. [CrossRef]
85. Zhang, X.; Ren, B.; Li, X.; Xu, Y.; Liu, B.; Yu, P.; Sun, Y.; Mei, D. Efficiently enhanced visible-light photocatalytic activity by in situ deposition of Ag@AgBr on g-C_3N_4/Fe_3O_4 magnetic heterogeneous materials. *Sep. Purif. Technol.* **2021**, *254*, 117596. [CrossRef]
86. Han, C.; Huang, G.; Zhu, D.; Hu, K. Facile synthesis of MoS_2/Fe_3O_4 nanocomposite with excellent Photo-Fenton-like catalytic performance. *Mater. Chem. Phys.* **2017**, *200*, 16–22. [CrossRef]
87. Li, W.; Wu, H. Sodium citrate functionalized reusable Fe_3O_4@TiO_2 photocatalyst for water purification. *Chem. Phys. Lett.* **2017**, *686*, 178–182. [CrossRef]
88. Liu, S.-H.; Lu, J.-S.; Yang, S.-W. Highly visible-light-responsive Cu_2O/rGO decorated with Fe_3O_4@SiO_2 nanoparticles as a magnetically recyclable photocatalyst. *Nanotechnology* **2018**, *29*, 305606. [CrossRef] [PubMed]
89. Ayadi, H.; Khaled, A.; Halladja, S.; Boudraa, I.; Rehimi, Z.; Chehimi, M.M. Fe_3O_4/MMT Fenton-like heterogeneous catalyst for the methylene blue degradation. *Desalination Water Treat.* **2022**, *260*, 179–186. [CrossRef]
90. Gao, P.; Song, Y.; Hao, M.; Zhu, A.; Yang, H.; Yang, S. An effective and magnetic Fe_2O_3-ZrO_2 catalyst for phenol degradation under neutral pH in the heterogeneous Fenton-like reaction. *Sep. Purif. Technol.* **2018**, *201*, 238–243. [CrossRef]
91. Chen, W.; He, D.; Huang, J.; Zhu, K.; Lei, L.; He, H.; Ai, Y. One-step synthesis of novel Fe/Fe_3O_4 embedded in N-doped graphite-like carbon nanosheets with the entangled CNTs to activate peroxymonosulfate for bisphenol a degradation. *Sep. Purif. Technol.* **2022**, *295*, 121172. [CrossRef]
92. Cui, X.; Zhang, S.-S.; Geng, Y.; Zhen, J.; Zhan, J.; Cao, C.; Ni, S.-Q. Synergistic catalysis by Fe_3O_4-biochar/peroxymonosulfate system for the removal of bisphenol a. *Sep. Purif. Technol.* **2021**, *276*, 119351. [CrossRef]
93. Ma, A.; Yang, W.; Gao, K.; Tang, J. Concave gold nano-arrows (AuCNAs) for efficient catalytic reduction of 4-nitrophenol. *Chemosphere* **2023**, *310*, 136800. [CrossRef] [PubMed]
94. Majumder, J.; Bhunia, T.; Gorai, S.; De, D.; Karmakar, P.; Gachhui, R. Efficient degradation of 4-nitrophenol and colorimetric detection of Fe (III) by biogenic silver nanoparticles of *Papiliotrema laurentii*. *Mater. Sci. Eng. B* **2023**, *296*, 116647. [CrossRef]
95. Niu, H.; Li, J.; Wang, X.; Qiang, Z.; Ren, J. Au-Fe_3O_4 decorated polydopamine hollow nanoparticles as high performance catalysts with magnetic responsive properties. *Nanotechnology* **2020**, *31*, 215606. [CrossRef] [PubMed]

96. Li, J.; Sun, X.; Subhan, S.; Gong, W.; Li, W.; Sun, W.; Zhang, Y.; Lu, M.; Ji, H.; Zhao, Z.; et al. Construction of novel Cu-based bimetal polycrystal@carbon catalyst prepared from bimetal HKUST-1 type MOFs (MOF-199s) for ultrafast reduction of 4-nitrophenol via interfacial synergistic catalysis. *Chem. Eng. J.* **2022**, *446*, 137314. [CrossRef]
97. Hu, C.; Yang, C.; Wang, X.; Wang, X.; Zhen, S.; Zhan, L.; Huang, C.; Li, Y. Rapid and facile synthesis of Au nanoparticle-decorated porous MOFs for the efficient reduction of 4-nitrophenol. *Sep. Purif. Technol.* **2022**, *300*, 121801. [CrossRef]
98. Vaiano, V.; Sacco, O.; Sannino, D.; Stoller, M.; Ciambelli, P.; Chianese, A. Photocatalytic removal of phenol by ferromagnetic N-TiO_2/SiO_2/Fe_3O_4 nanoparticles in presence of visible light irradiation. *Chem. Eng. Trans.* **2016**, *47*, 235–240. [CrossRef]
99. Shirgaonkar, I.Z.; Pandit, A.B. Sonophotochemical destruction of aqueous solution of 2,4,6-trichlorophenol. *Ultrason. Sonochem.* **1998**, *5*, 53–61. [CrossRef]
100. Gaya, U.I.; Abdullah, A.H.; Hussein, M.Z.; Zainal, Z. Photocatalytic removal of 2,4,6-trichlorophenol from water exploiting commercial ZnO powder. *Desalination* **2010**, *263*, 176–182. [CrossRef]
101. Huang, W.-J.; Fang, G.-C.; Wang, C.-C. A nanometer-ZnO catalyst to enhance the ozonation of 2,4,6-trichlorophenol in water. *Colloids Surf. A Physicochem. Eng. Asp.* **2005**, *260*, 45–51. [CrossRef]
102. Anandan, S.; Vinu, A.; Mori, T.; Gokulakrishnan, N.; Srinivasu, P.; Murugesan, V.; Ariga, K. Photocatalytic degradation of 2,4,6-trichlorophenol using lanthanum doped ZnO in aqueous suspension. *Catal. Commun.* **2007**, *8*, 1377–1382. [CrossRef]
103. Díaz-Díaz, G.; Celis-García, M.; Blanco-López, M.C.; Lobo-Castañón, M.J.; Miranda-Ordieres, A.J.; Tuñón-Blanco, P. Heterogeneous catalytic 2,4,6-trichlorophenol degradation at hemin–acrylic copolymer. *Appl. Catal. B Environ.* **2010**, *96*, 51–56. [CrossRef]
104. Teng, W.; Xu, J.; Yu, J.; Cong, S.; Yan, X. Experimental and quantum chemical investigation on the mechanism of photocatalytic degradation of 2,4,6-trichlorophenol by Ag/TiO_2 nanotube electrode. *J. Electroanal. Chem.* **2022**, *921*, 116662. [CrossRef]
105. Peng, H.; Cui, J.; Zhan, H.; Zhang, X. Improved photodegradation and detoxification of 2,4,6-trichlorophenol by lanthanum doped magnetic TiO_2. *Chem. Eng. J.* **2015**, *264*, 316–321. [CrossRef]
106. Li, L.; Guo, Q.; Lv, B.; Zheng, M.; Zhan, W.; Liu, Y.; Xu, W.; Wang, R.; Zeng, H.; Mao, B. Surface modified silver/magnetite nanocomposite activating hydrogen peroxide for efficient degradation of chlorophenols. *J. Colloid Interface Sci.* **2022**, *617*, 246–256. [CrossRef] [PubMed]
107. Choi, K.-H.; Min, J.; Park, S.-Y.; Park, B.J.; Jung, J.-S. Enhanced photocatalytic degradation of tri-chlorophenol by Fe_3O_4@TiO_2@Au photocatalyst under visible-light. *Ceram. Int.* **2019**, *45*, 9477–9482. [CrossRef]
108. Ghanbari, F.; Ahmadi, M.; Gohari, F. Heterogeneous activation of peroxymonosulfate via nanocomposite CeO_2-Fe_3O_4 for organic pollutants removal: The effect of UV and US irradiation and application for real wastewater. *Sep. Purif. Technol.* **2019**, *228*, 115732. [CrossRef]
109. Xu, L.; Wang, J. Degradation of 2,4,6-trichlorophenol using magnetic nanoscaled Fe_3O_4/CeO_2 composite as a heterogeneous Fenton-like catalyst. *Sep. Purif. Technol.* **2015**, *149*, 255–264. [CrossRef]
110. Liu, B.; Song, W.; Zhang, W.; Zhang, X.; Pan, S.; Wu, H.; Sun, Y.; Xu, Y. Fe_3O_4@CNT as a high-effective and steady chainmail catalyst for tetracycline degradation with peroxydisulfate activation: Performance and mechanism. *Sep. Purif. Technol.* **2021**, *273*, 118705. [CrossRef]
111. Mao, H.; Zhang, Q.; Cheng, F.; Feng, Z.; Hua, Y.; Zuo, S.; Cui, A.; Yao, C. Magnetically Separable Mesoporous Fe_3O_4@g-C_3N_4 as a Multifunctional Material for Metallic Ion Adsorption, Oil Removal from the Aqueous Phase, Photocatalysis, and Efficient Synergistic Photoactivated Fenton Reaction. *Ind. Eng. Chem. Res.* **2022**, *61*, 8895–8907. [CrossRef]
112. Moradi, M.; Kakavandi, B.; Bahadoran, A.; Giannakis, S.; Dehghanifard, E. Intensification of persulfate-mediated elimination of bisphenol A by a spinel cobalt ferrite-anchored g-C_3N_4S-scheme photocatalyst: Catalytic synergies and mechanistic interpretation. *Sep. Purif. Technol.* **2022**, *285*, 120313. [CrossRef]
113. Dadashi, J.; Khaleghian, M.; Mirtamizdoust, B.; Hanifehpour, Y.; Joo, S.W. Fabrication of Copper (II)-Coated Magnetic Core-Shell Nanoparticles Fe_3O_4@SiO_2: An Effective and Recoverable Catalyst for Reduction/Degradation of Environmental Pollutants. *Crystals* **2022**, *12*, 862. [CrossRef]
114. Hu, J.; Dong, Y.; Rahman, Z.; Ma, Y.; Ren, C.; Chen, X. In situ preparation of core-satellites nanostructural magnetic-Au NPs composite for catalytic degradation of organic contaminants. *Chem. Eng. J.* **2014**, *254*, 514–523. [CrossRef]
115. Kaushik, J.; Twinkle; Tisha; Nisha; Baig, A.; Sonal Dubey, P.; Sonkar, S.K. Photoactive Fe_3O_4@Fe_2O_3 Synthesized from Industrial Iron Oxide Dust for Fenton-Free Degradation of Multiple Organic Dye. *Ind. Eng. Chem. Res.* **2023**, *62*, 10487–10497. [CrossRef]
116. Lu, Y.; Xu, H.; Wei, S.; Jiang, F.; Zhang, J.; Ge, Y.; Li, Z. In situ doping lignin-derived carbon quantum dots on magnetic hydrotalcite for enhanced degradation of Congo Red over a wide pH range and simultaneous removal of heavy metal ions. *Int. J. Biol. Macromol.* **2023**, *239*, 124303. [CrossRef] [PubMed]

Disclaimer/Publisher's Note: The statements, opinions and data contained in all publications are solely those of the individual author(s) and contributor(s) and not of MDPI and/or the editor(s). MDPI and/or the editor(s) disclaim responsibility for any injury to people or property resulting from any ideas, methods, instructions or products referred to in the content.